



1  
2 **Mitochondrial respiratory states and rates:**  
3 **Building blocks of mitochondrial physiology Part 1**  
4

5 **COST Action CA15203 MitoEAGLE preprint** Version: 2018-09-04(41)

6 Corresponding author: Gnaiger E

7 Co-authors:

8 Aasander Frostner E, Abumrad NA, Acuna-Castroviejo D, Ahn B, Ali SS, Alves MG, Amati  
9 F, Amoedo ND, Aral C, Arandarçikaitè O, Bailey DM, Bajpeyi S, Bakker BM, Bastos  
10 Sant'Anna Silva AC, Battino M, Bazil J, Beard DA, Bednarczyk P, Ben-Shachar D, Bergdahl  
11 A, Bernardi P, Bishop D, Blier PU, Boetker HE, Boros M, Borsheim E, Borutaitè V,  
12 Bouillaud F, Bouitbir J, Breton S, Brown DA, Brown GC, Brown RA, Brozinick JT, Buettner  
13 GR, Burtscher J, Calabria E, Calbet JA, Calzia E, Cannon DT, Canto AC, Cardoso LHD,  
14 Carvalho E, Casado Pinna M, Cassina AM, Castro L, Cavalcanti-de-Albuquerque JP,  
15 Cervinkova Z, Chaurasia B, Chen Q, Chicco AJ, Chinopoulos C, Chowdhury SK, Clementi E,  
16 Coen PM, Coker RH, Collin A, Crisóstomo L, Di Marcello M, Darveau CA, Das AM, Dash  
17 RK, Davis MS, De Palma C, Dembinska-Kiec A, Dias TR, Distefano G, Doerrier C, Drahota  
18 Z, Dubouchaud H, Duchon MR, Dumas JF, Durham WJ, Dymkowska D, Dyrstad SE,  
19 Dzialowski EM, Ehinger J, Elmer E, Endlicher R, Engin AB, Fell DA, Ferko M, Ferreira  
20 JCB, Ferreira R, Fessel JP, Filipovska A, Fisar Z, Fischer M, Fisher G, Fisher JJ, Fornaro M,  
21 Galina A, Galkin A, Gan Z, Garcia-Roves PM, Garcia-Souza LF, Garipi E, Garlid KD,  
22 Garrabou G, Garten A, Gastaldelli A, Genova ML, Giovarelli M, Gonzalez-Armenta JL,  
23 Gonzalo H, Goodpaster BH, Gorr TA, Gourlay CW, Granata C, Grefte S, Gueguen N, Haas  
24 CB, Haavik J, Haendeler J, Hamann A, Han J, Hancock CR, Hand SC, Hargreaves IP,  
25 Harrison DK, Heales SJR, Hellgren KT, Hepple RT, Hernansanz-Agustin P, Hickey AJ, Hoel  
26 F, Holland OJ, Holloway GP, Hoppel CL, Houstek J, Hunger M, Iglesias-Gonzalez J, Irving  
27 BA, Iyer S, Jackson CB, Jadiya P, Jang DH, Jang YC, Jansen-Dürr P, Jarmuszkiewicz W,  
28 Jespersen NR, Jha RK, Jurk D, Kaambre T, Kaczor JJ, Kainulainen H, Kandel SM, Kane DA,  
29 Kappler L, Karabatsiakakis A, Karkucinska-Wieckowska A, Keijer J, Keppner G, Khamoui AV,  
30 Klingenspor M, Komlodi T, Koopman WJH, Kopitar-Jerala N, Kowaltowski AJ, Kozlov AV,  
31 Krajcova A, Krako Jakovljevic N, Kristal BS, Kuang J, Kucera O, Kwak HB, Kwast K,  
32 Labieniec-Watala M, Lai N, Land JM, Lane N, Laner V, Lanza IR, Larsen TS, Lavery GG,  
33 Lee HK, Leuwenburgh C, Lemieux H, Lerfall J, Li PA, Liu J, Lucchinetti E, Macedo MP,  
34 MacMillan-Crow LA, Makrecka-Kuka M, Malik A, Markova M, Martin DS, Mazat JP,  
35 McKenna HT, Menze MA, Meszaros AT, Methner A, Michalak S, Moellering DR, Moiso N,  
36 Molina AJA, Montaigne D, Moore AL, Moreau K, Moreno-Sánchez R, Moreira BP, Mracek  
37 T, Muntane J, Muntean DM, Murray AJ, Nair KS, Nemeč M, Neuffer PD, Neuzil J, Newsom  
38 S, Nozickova K, O'Brien KA, O'Gorman D, Oliveira MF, Oliveira MT, Oliveira PF, Oliveira  
39 PJ, Orynbayeva Z, Osiewacz HD, Pak YK, Pallotta ML, Palmeira CM, Parajuli N, Passos JF,  
40 Patel HH, Pecina P, Pelnen D, Pereira da Silva Grilo da Silva F, Perez Valencia JA, Pesta D,  
41 Petit PX, Pettersen IKN, Pichaud N, Piel S, Pietka TA, Pino MF, Pirkmajer S, Porter C, Porter  
42 RK, Pranger F, Prochownik EV, Pulinilkunnil T, Puskarich MA, Puurand M, Quijano C,  
43 Radenkovic F, Radi R, Ramzan R, Rattan S, Reboredo P, Rich PR, Renner-Sattler K, Rial E,  
44 Robinson MM, Roden M, Rodríguez-Enriquez S, Rohlena J, Rolo AP, Ropelle ER, Røslund  
45 GV, Rossignol R, Rossiter HB, Rybacka-Mossakowska J, Saada A, Safaei Z, Salin K,

46 Salvadego D, Sandi C, Sanz A, Sazanov LA, Scatena R, Schartner M, Scheibye-Knudsen M,  
 47 Schilling JM, Schlattner U, Schönfeld P, Schwarzer C, Scott GR, Shabalina IG, Sharma P,  
 48 Sharma V, Shevchuk I, Siewiera K, Silber AM, Silva AM, Sims CA, Singer D, Skolik R,  
 49 Smenes BT, Smith J, Soares FAA, Sobotka O, Sokolova I, Sonkar VK, Sowton AP, Sparagna  
 50 GC, Sparks LM, Spinazzi M, Stankova P, Stary C, Stiban J, Stier A, Stocker R, Sumbalova Z,  
 51 Suravajhala P, Swerdlow RH, Swiniuch D, Szabo I, Szewczyk A, Szibor M, Tanaka M,  
 52 Tandler B, Tarnopolsky MA, Tavernarakis N, Tepp K, Thyfault JP, Tomar D, Towheed A,  
 53 Tretter L, Trifunovic A, Trivigno C, Tronstad KJ, Trougakos IP, Tyrrell DJ, Urban T,  
 54 Valentine JM, Velika B, Vendelin M, Vercesi AE, Victor VM, Vieyra A Villena JA,  
 55 Vinogradov AD, Viscomi C, Vitorino RMP, Vogt S, Volani C, Votion DM, Vujacic-Mirski  
 56 K, Wagner BA, Ward ML, Warnsmann V, Wasserman DH, Watala C, Wei YH, Wieckowski  
 57 MR, Williams C, Wohlgemuth SE, Wohlwend M, Wolff J, Wüst RCI, Yokota T, Zablocki K,  
 58 Zaugg K, Zaugg M, Zhang Y, Zhang YZ, Zischka H, Zorzano A  
 59

### 60 Updates and discussion:

61 [http://www.mito eagle.org/index.php/MitoEAGLE\\_preprint\\_2018-02-08](http://www.mito eagle.org/index.php/MitoEAGLE_preprint_2018-02-08)

62 Correspondence: Gnaiger E

63 *Chair COST Action CA15203 MitoEAGLE* – <http://www.mito eagle.org>

64 *Department of Visceral, Transplant and Thoracic Surgery, D. Swarovski Research*  
 65 *Laboratory, Medical University of Innsbruck, Innrain 66/4, A-6020 Innsbruck, Austria*

66 *Email: mitoeagle@i-med.ac.at; Tel: +43 512 566796, Fax: +43 512 566796 20*  
 67

### 68 Abstract - Executive summary

69 **1. Introduction** – Box 1: In brief: Mitochondria and Bioblasts

70 **2. Coupling states and rates in mitochondrial preparations**

71 Mitochondrial preparations

72 *2.1. Respiratory control and coupling*

73 The steady-state

74 Specification of biochemical dose

75 Phosphorylation,  $P_{\gg}$ , and  $P_{\gg}/O_2$  ratio

76 Control and regulation

77 Respiratory control and response

78 Respiratory coupling control and ET-pathway control

79 Coupling

80 Uncoupling

81 *2.2. Coupling states and respiratory rates*

82 Respiratory capacities in coupling control states

83 LEAK, OXPHOS, ET, ROX

84 *2.3. Classical terminology for isolated mitochondria*

85 States 1–5

86 **3. What is a rate?** – Box 2: Metabolic flows and fluxes: vectorial, vectorial, and scalar

87 **4. Normalization of rate per sample**

88 *4.1. Flow: per object*

89 *4.2. Size-specific flux: per sample size*

90 *4.3. Marker-specific flux: per mitochondrial content*

91 **5. Normalization of rate per system**

92 *5.1. Flow: per chamber*

93 *5.2. Flux: per chamber volume*

94 **6. Conversion of units**

95 **7. Conclusions** – Box 3: Recommendations for studies with mitochondrial preparations

96 **References**

97

98 **Abstract** As the knowledge base and importance of mitochondrial physiology to human health  
99 expands, the necessity for harmonizing the terminology concerning mitochondrial respiratory  
100 states and rates has become increasingly apparent. The chemiosmotic theory establishes the  
101 mechanism of energy transformation and coupling in oxidative phosphorylation. The unifying  
102 concept of the protonmotive force provides the framework for developing a consistent  
103 theoretical foundation of mitochondrial physiology and bioenergetics. We follow IUPAC  
104 guidelines on terminology in physical chemistry, extended by considerations on open systems  
105 and thermodynamics of irreversible processes. The concept-driven constructive terminology  
106 incorporates the meaning of each quantity and aligns concepts and symbols to the nomenclature  
107 of classical bioenergetics. We endeavour to provide a balanced view on mitochondrial  
108 respiratory control and a critical discussion on reporting data of mitochondrial respiration in  
109 terms of metabolic flows and fluxes. Uniform standards for evaluation of respiratory states and  
110 rates will ultimately support the development of databases of mitochondrial respiratory function  
111 in species, tissues, and cells. Clarity of concept and consistency of nomenclature facilitate  
112 effective transdisciplinary communication, education, and ultimately further discovery.

113  
114 *Keywords:* Mitochondrial respiratory control, coupling control, mitochondrial  
115 preparations, protonmotive force, uncoupling, oxidative phosphorylation, OXPHOS,  
116 efficiency, electron transfer, ET; proton leak, LEAK, residual oxygen consumption, ROX, State  
117 2, State 3, State 4, normalization, flow, flux, O<sub>2</sub>

---

## 119 **Executive summary**

120  
121 In view of the broad implications for health care, mitochondrial researchers face an  
122 increasing responsibility to disseminate their fundamental knowledge and novel discoveries to  
123 a wide range of stakeholders and scientists beyond the group of specialists. This requires  
124 implementation of a commonly accepted terminology within the discipline and standardization  
125 in the translational context. Authors, reviewers, journal editors, and lecturers are challenged to  
126 collaborate with the aim to harmonize the nomenclature in the growing field of mitochondrial  
127 physiology and bioenergetics, from evolutionary biology and comparative physiology to  
128 mitochondrial medicine. In the present communication we focus on the following aspects of  
129 mitochondrial physiology:

- 130 1. Aerobic respiration depends on the coupling of phosphorylation (ADP → ATP) to O<sub>2</sub>  
131 flux in catabolic reactions. Coupling in oxidative phosphorylation is mediated by  
132 translocation of protons across the inner mitochondrial membrane through proton  
133 pumps generating or utilizing the protonmotive force, that is measured between the  
134 mitochondrial matrix and intermembrane compartment or outer mitochondrial  
135 space. Compartmental coupling distinguishes vectorial oxidative phosphorylation  
136 from glycolytic fermentation as the counterpart of cellular core energy metabolism  
137 (**Figure 1**). Cell respiration is distinguished from fermentation by: (1) Electron  
138 acceptors supplied by external respiration for the maintenance of redox balance,  
139 whereas fermentation is characterized by an internal electron acceptor produced in  
140 intermediary metabolism. In aerobic cell respiration, redox balance is maintained  
141 by O<sub>2</sub> as the electron acceptor. (2) Compartmental coupling in vectorial oxidative  
142 phosphorylation, in contrast to exclusively scalar substrate-level phosphorylation  
143 in fermentation.
- 144 2. To exclude fermentation and other cytosolic interactions from exerting an effect on the  
145 analysis of mitochondrial metabolism, the barrier function of the plasma membrane  
146 must be disrupted. Selective removal or permeabilization of the plasma membrane  
147 yields mitochondrial preparations—including isolated mitochondria, tissue and  
148 cellular preparations—with structural and functional integrity. Then extra-  
149 mitochondrial concentrations of fuel substrates, ADP, ATP, inorganic phosphate,

and cations including  $H^+$  can be controlled to determine mitochondrial function under a set of conditions defined as coupling control states. A concept-driven terminology of bioenergetics explicitly incorporates in its terms and symbols information on the nature of respiratory states that makes the technical terms readily recognized and easier to understand.

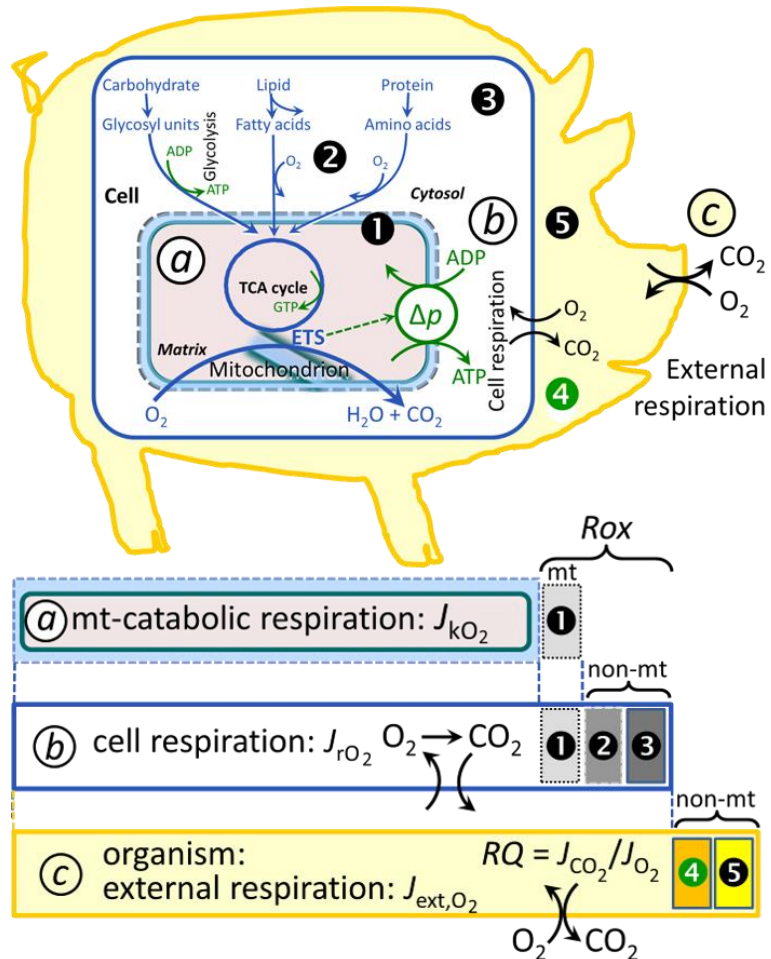
**Figure 1. Mitochondrial respiration is the oxidation of fuel substrates (electron donors) and reduction of  $O_2$  catalysed by the electron transfer system, ETS: (a) mitochondrial catabolic respiration; (b) total cellular  $O_2$  consumption; and (c) external respiration**

All chemical reactions,  $r$ , that consume  $O_2$  in the cells of an organism, contribute to cell respiration,  $J_{rO_2}$ . **1** Mitochondrial residual oxygen consumption,  $Rox$ . **2** Non-mitochondrial  $O_2$  consumption by catabolic reactions, particularly peroxisomal oxidases and microsomal cytochrome P450 systems. **3** Non-mitochondrial  $Rox$  by reactions unrelated to catabolism.  $mt-Rox$  and non- $mt Rox$  are measured without fuel substrate supply or after inhibiting the ETS. **4** Aerobic microbial respiration. **5** Extracellular  $O_2$  consumption. Bars are not at a quantitative scale.

**a Mitochondrial catabolic respiration**,  $J_{kO_2}$ , is the  $O_2$  consumption by the mitochondrial ETS excluding  $Rox$ .

**b Cell respiration**,  $J_{rO_2}$ , takes into account internal  $O_2$ -consuming reactions,  $r$ , including catabolic respiration and  $Rox$ . Catabolic cell respiration is the  $O_2$  consumption associated with catabolic pathways in the cell, including mitochondrial catabolism in addition to peroxisomal and microsomal oxidation reactions (**2**).

**c External respiration** balances internal respiration at steady-state, including aerobic respiration by the microbiome (**4**) and extracellular  $O_2$  consumption (**5**).  $O_2$  is transported from the environment across the respiratory cascade, *i.e.*, circulation between tissues and diffusion across cell membranes, to the intracellular compartment. The respiratory quotient,  $RQ$ , is the molar  $CO_2/O_2$  exchange ratio; when combined with the respiratory nitrogen quotient,  $N/O_2$  (mol N given off per mol  $O_2$  consumed), the  $RQ$  reflects the proportion of carbohydrate, lipid and protein utilized in cell respiration during aerobically balanced steady-states. Bicarbonate and  $CO_2$  are transported in reverse to the extracellular milieu and the organismic environment. Hemoglobin provides the molecular paradigm for the combination of  $O_2$  and  $CO_2$  exchange, as do lungs and gills on the morphological level.



- 200 3. Mitochondrial coupling states are defined according to the control of respiratory oxygen  
 201 flux by the protonmotive force. Capacities of oxidative phosphorylation and  
 202 electron transfer are measured at kinetically saturating concentrations of fuel  
 203 substrates, ADP and inorganic phosphate, and O<sub>2</sub>, or at optimal uncoupler  
 204 concentrations, respectively, in the absence of Complex IV inhibitors such as NO,  
 205 CO, or H<sub>2</sub>S. Respiratory capacity is a measure of the upper bound of the rate of  
 206 respiration, depends on the substrate type undergoing oxidation, and provides  
 207 reference values for the diagnosis of health and disease, and for evaluation of the  
 208 effects of Evolutionary background, Age, Gender and sex, Lifestyle and  
 209 Environment.
- 210 4. Incomplete tightness of coupling, *i.e.*, some degree of uncoupling relative to the  
 211 substrate-dependent coupling stoichiometry, is a characteristic of energy-  
 212 transformations across membranes. Uncoupling is caused by a variety of  
 213 physiological, pathological, toxicological, pharmacological and environmental  
 214 conditions that exert an influence not only on the proton leak and cation cycling,  
 215 but also on proton slip within the proton pumps and the structural integrity of the  
 216 mitochondria. A more loosely coupled state is induced by stimulation of  
 217 mitochondrial superoxide formation and the bypass of proton pumps. In addition,  
 218 uncoupling by application of protonophores represents an experimental  
 219 intervention for the transition from a well-coupled to the noncoupled state of  
 220 mitochondrial respiration.
- 221 5. Respiratory oxygen consumption rates have to be carefully normalized to enable meta-  
 222 analytic studies beyond the question of a particular experiment. Therefore, all raw  
 223 data should be published in a supplemental table or open access data repository.  
 224 Sample-specific normalization of rates for: (1) the number of objects (cells,  
 225 organisms); (2) the volume or mass of the experimental sample; and (3) the  
 226 concentration of mitochondrial markers in the experimental chamber is  
 227 distinguished from system-specific normalization for the volume of the chamber  
 228 (the measuring system).
- 229 6. The consistent use of terms and symbols will facilitate transdisciplinary communication  
 230 and support further developments of a database on bioenergetics and mitochondrial  
 231 physiology. The present considerations are focused on studies with mitochondrial  
 232 preparations. These will be extended in a series of reports on pathway control of  
 233 mitochondrial respiration, respiratory states in intact cells, and harmonization of  
 234 experimental procedures.

---

### 236 **Box 1: In brief – Mitochondria and Bioblasts**

237  
 238  
 239 *‘For the physiologist, mitochondria afforded the first opportunity for an*  
 240 *experimental approach to structure-function relationships, in particular those*  
 241 *involved in active transport, vectorial metabolism, and metabolic control*  
 242 *mechanisms on a subcellular level’ (Ernster and Schatz 1981).*

243 **Mitochondria** are the oxygen-consuming electrochemical generators evolved from  
 244 endosymbiotic bacteria (Margulis 1970; Lane 2005). They were described by Richard Altmann  
 245 (1894) as ‘bioblasts’, which include not only the mitochondria as presently defined, but also  
 246 symbiotic and free-living bacteria. The word ‘mitochondria’ (Greek mitos: thread; chondros:  
 247 granule) was introduced by Carl Benda (1898).

248 Mitochondria form dynamic networks within eukaryotic cells and are morphologically  
 249 enclosed by a double membrane. The mitochondrial inner membrane (mtIM) shows dynamic  
 250 tubular to disk-shaped cristae that separate the mitochondrial matrix, *i.e.*, the negatively charged  
 251 internal mitochondrial compartment, from the intermembrane space; the latter being enclosed

252 by the mitochondrial outer membrane (mtOM) and positively charged with respect to the  
253 matrix. The mtIM contains the non-bilayer phospholipid cardiolipin, which is not present in  
254 any other eukaryotic cellular membrane. Cardiolipin stabilizes and promotes the formation of  
255 respiratory supercomplexes (SC I<sub>n</sub>III<sub>n</sub>IV<sub>n</sub>), which are supramolecular assemblies based upon  
256 specific, though dynamic interactions between individual respiratory complexes (Greggio *et al.*  
257 2017; Lenaz *et al.* 2017). Membrane fluidity exerts an influence on functional properties of  
258 proteins incorporated in the membranes (Waczulikova *et al.* 2007). In addition to mitochondrial  
259 movement along microtubules, mitochondrial morphology can change in response to energy  
260 requirements of the cell via processes known as fusion and fission, through which mitochondria  
261 communicate within a network (Chan 2006). Intracellular stress factors may cause shrinking or  
262 swelling of the mitochondrial matrix, that can ultimately result in permeability transition.

263 Mitochondria are the structural and functional elementary components of cell respiration.  
264 Mitochondrial respiration is the reduction of molecular oxygen by electron transfer coupled to  
265 electrochemical proton translocation across the mtIM. In the process of oxidative  
266 phosphorylation (OXPHOS), the catabolic reaction of oxygen consumption is  
267 electrochemically coupled to the transformation of energy in the form of adenosine triphosphate  
268 (ATP; Mitchell 1961, 2011). Mitochondria are the powerhouses of the cell which contain the  
269 machinery of the OXPHOS-pathways, including transmembrane respiratory complexes (proton  
270 pumps with FMN, Fe-S and cytochrome *b*, *c*, *aa3* redox systems); alternative dehydrogenases  
271 and oxidases; the coenzyme ubiquinone (Q); F-ATPase or ATP synthase; the enzymes of the  
272 tricarboxylic acid cycle, fatty acid and amino acid oxidation; transporters of ions, metabolites  
273 and co-factors; iron/sulphur cluster synthesis; and mitochondrial kinases related to energy  
274 transfer pathways. The mitochondrial proteome comprises over 1,200 proteins (Calvo *et al.*  
275 2015; 2017), mostly encoded by nuclear DNA (nDNA), with a variety of functions, many of  
276 which are relatively well known (*e.g.*, proteins regulating mitochondrial biogenesis or  
277 apoptosis), while others are still under investigation, or need to be identified (*e.g.*, alanine  
278 transporter). Only recently has it been possible to use the mammalian mitochondrial proteome  
279 to discover and characterize the genetic basis of mitochondrial diseases (Williams *et al.* 2016;  
280 Palmfeldt and Bross 2017).

281 Mitochondria can traverse cell boundaries in a process known as horizontal mitochondrial  
282 transfer (Torralba *et al.* 2016). There is a constant crosstalk between mitochondria and the other  
283 cellular components. The crosstalk between mitochondria and endoplasmic reticulum is  
284 involved in the regulation of calcium homeostasis, cell division, autophagy, differentiation, and  
285 anti-viral signaling (Murley and Nunnari 2016). Mitochondria contribute to the formation of  
286 peroxisomes, which are hybrids of mitochondrial and ER-derived precursors (Sugiura *et al.*  
287 2017). Cellular mitochondrial homeostasis (mitostasis) is maintained through regulation at  
288 transcriptional, post-translational and epigenetic levels. Cell signalling modules contribute to  
289 homeostatic regulation throughout the cell cycle or even cell death by activating proteostatic  
290 modules (*e.g.*, the ubiquitin-proteasome and autophagy-lysosome/vacuole pathways; specific  
291 proteases like LON) and genome stability modules in response to varying energy demands and  
292 stress cues (Quiros *et al.* 2016). Acetylation is a post-translational modification capable of  
293 influencing the bioenergetic response, with clinically significant implications for health and  
294 disease (Carrico *et al.* 2018).

295 Mitochondria typically maintain several copies of their own circular genome known as  
296 mitochondrial DNA (mtDNA; hundred to thousands per cell; Cummins 1998), which is  
297 maternally inherited in humans. Biparental mitochondrial inheritance is documented in  
298 mammals, birds, fish, reptiles and invertebrate groups, and is even the norm in some bivalve  
299 taxonomic groups (Breton *et al.* 2007; White *et al.* 2008). The mitochondrial genome of the  
300 angiosperm *Amborella* contains a record of six mitochondrial genome equivalents acquired by  
301 horizontal transfer of entire genomes, two from angiosperms, three from algae and one from  
302 mosses (Rice *et al.* 2016). However, some organisms such as *Cryptosporidium* species have

303 morphologically and functionally reduced mitochondria without DNA (Liu *et al.* 2016). In  
304 vertebrates but not all invertebrates, mtDNA is compact (16.5 kB in humans) and encodes 13  
305 protein subunits of the transmembrane respiratory Complexes CI, CIII, CIV and F-ATPase, 22  
306 tRNAs, and two RNAs. Additional gene content has been suggested to include microRNAs,  
307 piRNA, smithRNAs, repeat associated RNA, and even additional proteins (Duarte *et al.* 2014;  
308 Lee *et al.* 2015; Cobb *et al.* 2016). The mitochondrial genome requires nuclear-encoded  
309 mitochondrially targeted proteins, *e.g.*, TFAM, for its maintenance and expression (Rackham  
310 *et al.* 2012). Both genomes encode peptides of the membrane spanning redox pumps (CI, CIII  
311 and CIV) and F-ATPase, leading to strong constraints in the coevolution of both genomes (Blier  
312 *et al.* 2001).

313 Mitochondrial dysfunction is associated with a wide variety of genetic and degenerative  
314 diseases. Robust mitochondrial function is supported by physical exercise and caloric balance,  
315 and is central for sustained metabolic health throughout life. Therefore, a more consistent  
316 presentation of mitochondrial physiology will improve our understanding of the etiology of  
317 disease, the diagnostic repertoire of mitochondrial medicine, with a focus on protective  
318 medicine, lifestyle and healthy aging.

319 Abbreviation: mt, as generally used in mtDNA. Mitochondrion is singular and  
320 mitochondria is plural.

321

322

## 323 1. Introduction

324

325 Mitochondria are the powerhouses of the cell with numerous physiological, molecular,  
326 and genetic functions (**Box 1**). Every study of mitochondrial health and disease is faced with  
327 Evolution, Age, Gender and sex, Lifestyle, and Environment (MitoEAGLE) as essential  
328 background conditions intrinsic to the individual person or cohort, species, tissue and to some  
329 extent even cell line. As a large and coordinated group of laboratories and researchers, the  
330 mission of the global MitoEAGLE Network is to generate the necessary scale, type, and quality  
331 of consistent data sets and conditions to address this intrinsic complexity. Harmonization of  
332 experimental protocols and implementation of a quality control and data management system  
333 are required to interrelate results gathered across a spectrum of studies and to generate a  
334 rigorously monitored database focused on mitochondrial respiratory function. In this way,  
335 researchers from a variety of disciplines can compare their findings using clearly defined and  
336 accepted international standards.

337 Reliability and comparability of quantitative results depend on the accuracy of  
338 measurements under strictly-defined conditions. A conceptual framework is required to warrant  
339 meaningful interpretation and comparability of experimental outcomes carried out by research  
340 groups at different institutes. With an emphasis on quality of research, collected data can be  
341 useful far beyond the specific question of a particular experiment. Standardization and  
342 homogenization of terminology, methodology, and data sets could lead to the development of  
343 open-access databases such as those that have been developed for National Institutes of Health  
344 sponsored research in genetics, proteomics, and metabolomics. Enabling meta-analytic studies  
345 is the most economic way of providing robust answers to biological questions (Cooper *et al.*  
346 2009). Vague or ambiguous jargon can lead to confusion and may relegate valuable signals to  
347 wasteful noise. For this reason, measured values must be expressed in standard units for each  
348 parameter used to define mitochondrial respiratory function. Harmonization of nomenclature  
349 and definition of technical terms are essential to improve the awareness of the intricate meaning  
350 of current and past scientific vocabulary, for documentation and integration into databases in  
351 general, and quantitative modelling in particular (Beard 2005). The focus on coupling states  
352 and fluxes through metabolic pathways of aerobic energy transformation in mitochondrial  
353 preparations is a first step in the attempt to generate a conceptually-oriented nomenclature in

354 bioenergetics and mitochondrial physiology. Coupling states of intact cells, the protonmotive  
355 force, and respiratory control by fuel substrates and specific inhibitors of respiratory enzymes  
356 will be reviewed in subsequent communications, prepared In the frame of COST Action  
357 MitoEAGLE open to global bottom-up input.

358  
359

## 360 **2. Coupling states and rates in mitochondrial preparations**

361 *‘Every professional group develops its own technical jargon for talking about matters of*  
362 *critical concern ... People who know a word can share that idea with other members of*  
363 *their group, and a shared vocabulary is part of the glue that holds people together and*  
364 *allows them to create a shared culture’ (Miller 1991).*

365

366 **Mitochondrial preparations** are defined as either isolated mitochondria, or tissue and  
367 cellular preparations in which the barrier function of the plasma membrane is disrupted. Since  
368 this entails the loss of cell viability, mitochondrial preparations are not studied *in vivo*. In  
369 contrast to isolated mitochondria and tissue homogenate preparations, mitochondria in  
370 permeabilized tissues and cells are *in situ* relative to the plasma membrane. The plasma  
371 membrane separates the intracellular compartment including the cytosol, nucleus, and  
372 organelles from the extracellular environment. The plasma membrane consists of a lipid bilayer  
373 with embedded proteins and attached organic molecules that collectively control the selective  
374 permeability of ions, organic molecules, and particles across the cell boundary. The intact  
375 plasma membrane prevents the passage of many water-soluble mitochondrial substrates and  
376 inorganic ions—such as succinate, adenosine diphosphate (ADP) and inorganic phosphate ( $P_i$ ),  
377 that must be controlled at kinetically-saturating concentrations for the analysis of respiratory  
378 capacities. Despite the activity of solute carriers, *e.g.*, SLC13A3 and SLC20A2, that transport  
379 these metabolites across the plasma membrane of various cell types, this limits the scope of  
380 investigations into mitochondrial respiratory function in intact cells (**Figure 2A**).

381 The cholesterol content of the plasma membrane is high compared to mitochondrial  
382 membranes (Korn 1969). Therefore, mild detergents—such as digitonin and saponin—can be  
383 applied to selectively permeabilize the plasma membrane by interaction with cholesterol and  
384 allow free exchange of organic molecules and inorganic ions between the cytosol and the  
385 immediate cell environment, while maintaining the integrity and localization of organelles,  
386 cytoskeleton, and the nucleus. Application of optimum concentrations of permeabilization  
387 agents (mild detergents or toxins) leads to washout of cytosolic marker enzymes—such as  
388 lactate dehydrogenase—and results in the complete loss of cell viability, tested by nuclear  
389 staining using membrane-impermeable dyes, while mitochondrial function remains intact,  
390 tested by cytochrome *c* addition, for example. Respiration of isolated mitochondria remains  
391 unaltered after the addition of low concentrations of digitonin or saponin, although care should  
392 be taken when isolating mitochondria from cancer cells since they have significantly higher  
393 contents of cholesterol in both membranes (Baggetto and Testa-Perussini, 1990). In addition to  
394 mechanical cell disruption during homogenization of tissue, permeabilization agents may be  
395 applied to ensure permeabilization of all cells in tissue homogenates. Suspensions of cells  
396 permeabilized in the respiration chamber and crude tissue homogenates contain all components  
397 of the cell at highly dilute concentrations. All mitochondria are retained in chemically-  
398 permeabilized mitochondrial preparations and crude tissue homogenates. In the preparation of  
399 isolated mitochondria, however, the mitochondria are separated from other cell fractions and  
400 purified by differential centrifugation, entailing the loss of a fraction of the total mitochondrial  
401 content. Typical mitochondrial recovery ranges from 30% to 80%. Using Percoll or sucrose  
402 density gradients to maximize the purity of isolated mitochondria may compromise the  
403 mitochondrial yield or structural and functional integrity. Therefore, protocols to isolate  
404 mitochondria need to be optimized according to each study. The term mitochondrial preparation



405 does neither include further fractionation of mitochondrial components, nor submitochondrial  
406 particles.

407

### 408 2.1. Respiratory control and coupling

409

410 Respiratory coupling control states are established in studies of mitochondrial  
411 preparations to obtain reference values for various output variables (**Table 1**). Physiological  
412 conditions *in vivo* deviate from these experimentally obtained states. Since kinetically-  
413 saturating concentrations, *e.g.*, of ADP or oxygen (O<sub>2</sub>; dioxygen), may not apply to  
414 physiological intracellular conditions, relevant information is obtained in studies of kinetic  
415 responses to variations in [ADP] or [O<sub>2</sub>] in the range between kinetically-saturating  
416 concentrations and anoxia (Gnaiger 2001).

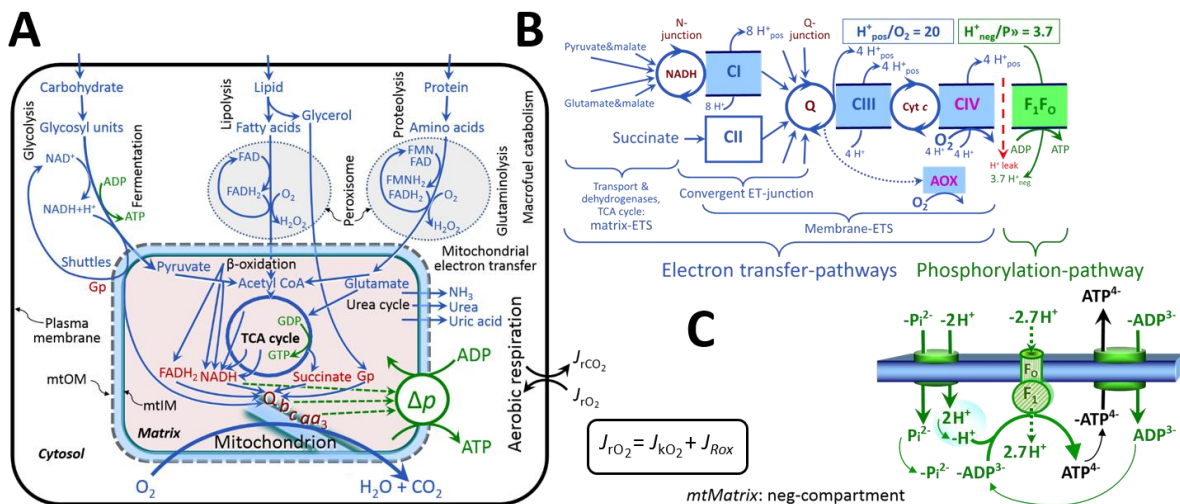
417 **The steady-state:** Mitochondria represent a thermodynamically open system in non-  
418 equilibrium states of biochemical energy transformation. State variables (protonmotive force;  
419 redox states) and metabolic *rates* (fluxes) are measured in defined mitochondrial respiratory  
420 *states*. Steady-states can be obtained only in open systems, in which changes by *internal*  
421 transformations, *e.g.*, O<sub>2</sub> consumption, are instantaneously compensated for by *external* fluxes,  
422 *e.g.*, O<sub>2</sub> supply, preventing a change of O<sub>2</sub> concentration in the system (Gnaiger 1993b).  
423 Mitochondrial respiratory states monitored in closed systems satisfy the criteria of pseudo-  
424 steady states for limited periods of time, when changes in the system (concentrations of O<sub>2</sub>, fuel  
425 substrates, ADP, P<sub>i</sub>, H<sup>+</sup>) do not exert significant effects on metabolic fluxes (respiration,  
426 phosphorylation). Such pseudo-steady states require respiratory media with sufficient buffering  
427 capacity and substrates maintained at kinetically-saturating concentrations, and thus depend on  
428 the kinetics of the processes under investigation.

429 **Specification of biochemical dose:** Substrates, uncouplers, inhibitors, and other  
430 chemical reagents are titrated to dissect mitochondrial function. Nominal concentrations of  
431 these substances are usually reported as initial amount of substance concentration [mol·L<sup>-1</sup>] in  
432 the incubation medium. When aiming at the measurement of kinetically saturated processes—  
433 such as OXPHOS-capacities, the concentrations for substrates can be chosen according to the  
434 apparent equilibrium constant,  $K_m'$ . In the case of hyperbolic kinetics, only 80% of maximum  
435 respiratory capacity is obtained at a substrate concentration of four times the  $K_m'$ , whereas  
436 substrate concentrations of 5, 9, 19 and 49 times the  $K_m'$  are theoretically required for reaching  
437 83%, 90%, 95% or 98% of the maximal rate (Gnaiger 2001). Other reagents are chosen to  
438 inhibit or alter some processes. The amount of these chemicals in an experimental incubation  
439 is selected to maximize effect, avoiding unacceptable off-target consequences that would  
440 adversely affect the data being sought. Specifying the amount of substance in an incubation as  
441 nominal concentration in the aqueous incubation medium can be ambiguous (Doskey *et al.*  
442 2015), particularly for lipophilic substances (oligomycin, uncouplers, permeabilization agents)  
443 or cations (TPP<sup>+</sup>; fluorescent dyes such as safranin, TMRM; Chowdhury *et al.* 2015), which  
444 accumulate in biological membranes or in the mitochondrial matrix. For example, a dose of  
445 digitonin of 8 fmol·cell<sup>-1</sup> (10 pg·cell<sup>-1</sup>; 10 µg·10<sup>-6</sup> cells) is optimal for permeabilization of  
446 endothelial cells, and the concentration in the incubation medium has to be adjusted according  
447 to the cell density applied (Doerrier *et al.* 2018).

448 Generally, dose/exposure can be specified per unit of biological sample, *i.e.*, (nominal  
449 moles of xenobiotic)/(number of cells) [mol·cell<sup>-1</sup>] or, as appropriate, per mass of biological  
450 sample [mol·kg<sup>-1</sup>]. This approach to specification of dose/exposure provides a scalable  
451 parameter that can be used to design experiments, help interpret a wide variety of experimental  
452 results, and provide absolute information that allows researchers worldwide to make the most  
453 use of published data (Doskey *et al.* 2015).

454 **Phosphorylation, P<sub>»</sub>, and P<sub>»</sub>/O<sub>2</sub> ratio:** *Phosphorylation* in the context of OXPHOS is  
455 defined as phosphorylation of ADP by P<sub>i</sub> to form ATP. On the other hand, the term

456 phosphorylation is used generally in many contexts, *e.g.*, protein phosphorylation. This justifies  
 457 consideration of a symbol more discriminating and specific than P as used in the P/O ratio  
 458 (phosphate to atomic oxygen ratio), where P indicates phosphorylation of ADP to ATP or GDP  
 459 to GTP (**Figure 2**). We propose the symbol P» for the endergonic (uphill) direction of  
 460 phosphorylation ADP→ATP, and likewise the symbol P« for the corresponding exergonic  
 461 (downhill) hydrolysis ATP→ADP (**Figure 3**). P» refers mainly to electrontransfer  
 462 phosphorylation but may also involve substrate-level phosphorylation as part of the  
 463 tricarboxylic acid (TCA) cycle (succinyl-CoA ligase; phosphoglycerate kinase) and  
 464 phosphorylation of ADP catalyzed by pyruvate kinase, and of GDP phosphorylated by  
 465 phosphoenolpyruvate carboxykinase. Transphosphorylation is performed by adenylate kinase,  
 466 creatine kinase (mtCK), hexokinase and nucleoside diphosphate kinase. In isolated mammalian  
 467 mitochondria, ATP production catalyzed by adenylate kinase (2 ADP ↔ ATP + AMP) proceeds  
 468 without fuel substrates in the presence of ADP (Komlódi and Tretter 2017). Kinase cycles are  
 469 involved in intracellular energy transfer and signal transduction for regulation of energy flux.  
 470



471

472

## Figure 2. Cell respiration and oxidative phosphorylation (OXPHOS)

473

Mitochondrial respiration is the oxidation of fuel substrates (electron donors) with electron transfer to O<sub>2</sub> as the electron acceptor. For explanation of symbols see also **Figure 1**.

474

(A) Respiration of intact cells: Extra-mitochondrial catabolism of macrofuels or uptake of small molecules by the cell provides the *mitochondrial* fuel substrates. Many fuel substrates are catabolized to acetyl-CoA or to glutamate, and further electron transfer reduces nicotinamide adenine dinucleotide to NADH or flavin adenine dinucleotide to FADH<sub>2</sub>. In respiration, electron transfer is coupled to the phosphorylation of ADP to ATP, with energy transformation mediated by the protonmotive force,  $\Delta p$ . Anabolic reactions are linked to catabolism, both by ATP as the intermediary energy currency and by small organic precursor molecules as building blocks for biosynthesis (not shown). Glycolysis involves substrate-level phosphorylation of ADP to ATP in fermentation without utilization of O<sub>2</sub>. In contrast, extra-mitochondrial oxidation of fatty acids and amino acids proceeds partially in peroxisomes without coupling to ATP production: acyl-CoA oxidase catalyzes the oxidation of FADH<sub>2</sub> with electron transfer to O<sub>2</sub>; amino acid oxidases oxidize flavin mononucleotide FMNH<sub>2</sub> or FADH<sub>2</sub>. Coenzyme Q, Q, and the cytochromes *b*, *c*, and *aa*<sub>3</sub> are redox systems of the mitochondrial inner membrane, mtIM. Dashed arrows indicate the connection between the redox proton pumps (respiratory Complexes CI, CIII and CIV) and the transmembrane  $\Delta p$ . Mitochondrial outer membrane, mtOM; glycerol-3-phosphate, Gp; tricarboxylic acid cycle, TCA cycle.

475

476

477

478

479

480

481

482

483

484

485

486

487

488

489

490

(B) Respiration in mitochondrial preparations: The mitochondrial electron transfer system (ETS) is (1) fuelled by diffusion and transport of substrates across the mitochondrial outer and inner membrane, and in addition consists of the (2) matrix-ETS, and (3) membrane-ETS.

491

492

493

494 Upstream sections of ET-pathways converge at the N-junction. NADH mainly generated in the  
 495 TCA cycle is oxidized by CI and electron entry into the Q-junction. Similarly, succinate is  
 496 formed in the TCA cycle and oxidized by CII to fumarate. CII is part of both the TCA cycle  
 497 and the ETS, and reduces FAD to FADH<sub>2</sub> with further reduction of ubiquinone to ubiquinol  
 498 downstream of the TCA cycle in the Q-junction. Thus FADH<sub>2</sub> is not a substrate but is the  
 499 product of CII, in contrast to erroneous metabolic maps shown in many textbooks and  
 500 publications. Unspecified arrows converging at the Q-junction indicate additional ET-sections  
 501 with electron entry into Q through electron transferring flavoprotein, glycerophosphate  
 502 dehydrogenase, dihydro-orotate dehydrogenase, proline dehydrogenase, choline  
 503 dehydrogenase, and sulfide-ubiquinone oxidoreductase. The dotted arrow indicates the  
 504 branched pathway of oxygen consumption by alternative quinol oxidase (AOX). ET-pathways  
 505 are coupled to the phosphorylation-pathway. The H<sup>+</sup><sub>pos</sub>/O<sub>2</sub> ratio is the outward proton flux from  
 506 the matrix space to the positively (pos) charged vesicular compartment, divided by catabolic  
 507 O<sub>2</sub> flux in the NADH-pathway. The H<sup>+</sup><sub>neg</sub>/P<sub>»</sub> ratio is the inward proton flux from the inter-  
 508 membrane space to the negatively (neg) charged matrix space, divided by the flux of  
 509 phosphorylation of ADP to ATP. These stoichiometries are not fixed due to ion leaks and proton  
 510 slip. Modified from (B) Lemieux *et al.* (2017) and Rich (2013).

511 (C) Chemiosmotic phosphorylation-pathway catalyzed by the proton pump F<sub>1</sub>F<sub>0</sub>-ATPase (F-  
 512 ATPase, ATP synthase), adenine nucleotide translocase, and inorganic phosphate transporter.  
 513 The H<sup>+</sup><sub>neg</sub>/P<sub>»</sub> stoichiometry is the sum of the coupling stoichiometry in the F-ATPase reaction  
 514 (-2.7 H<sup>+</sup><sub>pos</sub> from the positive intermembrane space, 2.7 H<sup>+</sup><sub>neg</sub> to the matrix, *i.e.*, the negative  
 515 compartment) and the proton balance in the translocation of ADP<sup>3-</sup>, ATP<sup>4-</sup> and P<sub>i</sub><sup>2-</sup>. Modified  
 516 from Gnaiger (2014).

517  
 518 The P<sub>»</sub>/O<sub>2</sub> ratio (P<sub>»</sub>/4 e<sup>-</sup>) is two times the ‘P/O’ ratio (P<sub>»</sub>/2 e<sup>-</sup>) of classical bioenergetics.  
 519 P<sub>»</sub>/O<sub>2</sub> is a generalized symbol, not specific for determination of P<sub>i</sub> consumption (P<sub>i</sub>/O<sub>2</sub> flux  
 520 ratio), ADP depletion (ADP/O<sub>2</sub> flux ratio), or ATP production (ATP/O<sub>2</sub> flux ratio). The  
 521 mechanistic P<sub>»</sub>/O<sub>2</sub> ratio—or P<sub>»</sub>/O<sub>2</sub> stoichiometry—is calculated from the proton-to-O<sub>2</sub> and  
 522 proton-to-phosphorylation coupling stoichiometries (**Figure 2B**):  
 523

$$524 \quad P_{\gg}/O_2 = \frac{H_{\text{pos}}^+/O_2}{H_{\text{neg}}^+/P_{\gg}} \quad (1)$$

525  
 526 The H<sup>+</sup><sub>pos</sub>/O<sub>2</sub> *coupling stoichiometry* (referring to the full 4 electron reduction of O<sub>2</sub>) depends  
 527 on the relative involvement of the three coupling sites (respiratory Complexes I, III and IV; CI,  
 528 CIII and CIV) in the catabolic ET-pathway from reduced fuel substrates (electron donors) to  
 529 the reduction of O<sub>2</sub> (electron acceptor). This varies with: (1) a bypass of CI by single or multiple  
 530 electron input into the Q-junction; and (2) a bypass of CIV by involvement of alternative  
 531 oxidases, AOX, which are not expressed in mammalian mitochondria.

532 H<sup>+</sup><sub>pos</sub>/O<sub>2</sub> is 12 in the ET-pathways involving CIII and CIV as proton pumps, increasing to  
 533 20 for the NADH-pathway through CI (**Figure 2B**), but a general consensus on H<sup>+</sup><sub>pos</sub>/O<sub>2</sub>  
 534 stoichiometries remains to be reached (Hinkle 2005; Wikström and Hummer 2012; Sazanov  
 535 2015). The H<sup>+</sup><sub>neg</sub>/P<sub>»</sub> coupling stoichiometry (3.7; **Figure 2B**) is the sum of 2.7 H<sup>+</sup><sub>neg</sub> required  
 536 by the F-ATPase of vertebrate and most invertebrate species (Watt *et al.* 2010) and the proton  
 537 balance in the translocation of ADP, ATP and P<sub>i</sub> (**Figure 2C**). Taken together, the mechanistic  
 538 P<sub>»</sub>/O<sub>2</sub> ratio is calculated at 5.4 and 3.3 for NADH- and succinate-linked respiration,  
 539 respectively (Eq. 1). The corresponding classical P<sub>»</sub>/O ratios (referring to the 2 electron  
 540 reduction of 0.5 O<sub>2</sub>) are 2.7 and 1.6 (Watt *et al.* 2010), in agreement with the measured P<sub>»</sub>/O  
 541 ratio for succinate of 1.58 ± 0.02 (Gnaiger *et al.* 2000).

542 The effective P<sub>»</sub>/O<sub>2</sub> flux ratio ( $\dot{Y}_{P_{\gg}/O_2} = J_{P_{\gg}}/J_{kO_2}$ ; **Figure 3**) is diminished relative to the  
 543 mechanistic P<sub>»</sub>/O<sub>2</sub> ratio by intrinsic and extrinsic uncoupling *versus* dyscoupling (**Figure 4**).  
 544 Such generalized uncoupling is different from switching to mitochondrial pathways that involve

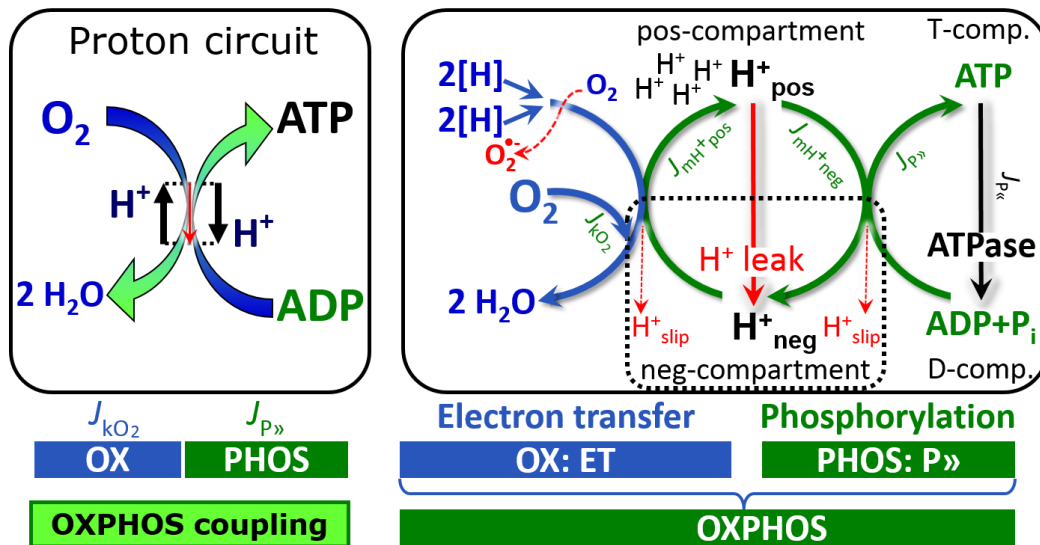
545 fewer than three proton pumps ('coupling sites': Complexes CI, CIII and CIV), bypassing CI  
 546 through multiple electron entries into the Q-junction, or CIII and CIV through AOX (**Figure**  
 547 **2B**). Reprogramming of mitochondrial pathways leading to different types of substrates being  
 548 oxidized may be considered as a switch of gears (changing the stoichiometry by altering the  
 549 substrate that is oxidized) rather than uncoupling (loosening the tightness of coupling relative  
 550 to a fixed stoichiometry). In addition,  $Y_{P\gg O_2}$  depends on several experimental conditions of flux  
 551 control, increasing as a hyperbolic function of [ADP] to a maximum value (Gnaiger 2001).

552 **Control and regulation:** The terms metabolic *control* and *regulation* are frequently used  
 553 synonymously, but are distinguished in metabolic control analysis: 'We could understand the  
 554 regulation as the mechanism that occurs when a system maintains some variable constant over  
 555 time, in spite of fluctuations in external conditions (homeostasis of the internal state). On the  
 556 other hand, metabolic control is the power to change the state of the metabolism in response to  
 557 an external signal' (Fell 1997). Respiratory control may be induced by experimental control  
 558 signals that *exert* an influence on: (1) ATP demand and ADP phosphorylation-rate; (2) fuel  
 559 substrate composition, pathway competition; (3) available amounts of substrates and O<sub>2</sub>, *e.g.*,  
 560 starvation and hypoxia; (4) the protonmotive force, redox states, flux–force relationships,  
 561 coupling and efficiency; (5) Ca<sup>2+</sup> and other ions including H<sup>+</sup>; (6) inhibitors, *e.g.*, nitric oxide  
 562 or intermediary metabolites such as oxaloacetate; (7) signalling pathways and regulatory  
 563 proteins, *e.g.*, insulin resistance, transcription factor hypoxia inducible factor 1. *Mechanisms* of  
 564 respiratory control and regulation include adjustments of: (1) enzyme activities by allosteric  
 565 mechanisms and phosphorylation; (2) enzyme content, concentrations of cofactors and  
 566 conserved moieties—such as adenylates, nicotinamide adenine dinucleotide [NAD<sup>+</sup>/NADH],  
 567 coenzyme Q, cytochrome *c*; (3) metabolic channeling by supercomplexes; and (4)  
 568 mitochondrial density (enzyme concentrations and membrane area) and morphology (cristae  
 569 folding, fission and fusion). Mitochondria are targeted directly by hormones, *e.g.*, progesterone  
 570 and glucacorticoids, which affect their energy metabolism (Lee *et al.* 2013; Gerö and Szabo  
 571 2016; Price and Dai 2016; Moreno *et al.* 2017). Evolutionary or acquired differences in the  
 572 genetic and epigenetic basis of mitochondrial function (or dysfunction) between individuals;  
 573 age; gender, biological sex, and hormone concentrations; life style including exercise and  
 574 nutrition; and environmental issues including thermal, atmospheric, toxic and pharmacological  
 575 factors, exert an influence on all control mechanisms listed above. For reviews, see Brown  
 576 1992; Gnaiger 1993a, 2009; 2014; Paradies *et al.* 2014; Morrow *et al.* 2017.

577 **Respiratory control and response:** Lack of control by a metabolic pathway, *e.g.*,  
 578 phosphorylation-pathway, means that there will be no response to a variable activating it, *e.g.*,  
 579 [ADP]. The reverse, however, is not true as the absence of a response to [ADP] does not exclude  
 580 the phosphorylation-pathway from having some degree of control. The degree of control of a  
 581 component of the OXPHOS-pathway on an output variable—such as O<sub>2</sub> flux, will in general  
 582 be different from the degree of control on other outputs—such as phosphorylation-flux or  
 583 proton leak flux. Therefore, it is necessary to be specific as to which input and output are under  
 584 consideration (Fell 1997).

585 **Respiratory coupling control and ET-pathway control:** Respiratory control refers to  
 586 the ability of mitochondria to adjust O<sub>2</sub> flux in response to external control signals by engaging  
 587 various mechanisms of control and regulation. Respiratory control is monitored in a  
 588 mitochondrial preparation under conditions defined as respiratory states, preferentially under  
 589 near-physiological conditions of O<sub>2</sub> concentration, pH, temperature and medium ionic  
 590 composition, to generate data of higher biological relevance. When phosphorylation of ADP to  
 591 ATP is stimulated or depressed, an increase or decrease is observed in electron transfer  
 592 measured as O<sub>2</sub> flux in respiratory coupling states of intact mitochondria ('controlled states' in  
 593 the classical terminology of bioenergetics). Alternatively, coupling of electron transfer with  
 594 phosphorylation is disengaged by uncouplers. These protonophores are weak lipid-soluble acids  
 595 which disrupt the barrier function of the mtIM and thus short circuit the protonmotive system,

596 functioning like a clutch in a mechanical system. The corresponding coupling control state is  
 597 characterized by a high  $O_2$  flux without control by  $P_{\gg}$  (noncoupled or ‘uncontrolled state’).  
 598  
 599



600 **Figure 3. Coupling in oxidative phosphorylation (OXPHOS)**  
 601  $2[H]$  indicates the reduced hydrogen equivalents of fuel substrates of the catabolic reaction  $k$   
 602 with oxygen.  $O_2$  flux,  $J_{kO_2}$ , through the catabolic ET-pathway, is coupled to flux through the  
 603 phosphorylation-pathway of ADP to ATP,  $J_{P_{\gg}}$ . The redox proton pumps of the ET-pathway  
 604 drive proton flux into the positive (pos) compartment,  $J_{mH^{+}pos}$ , generating the output  
 605 protonmotive force (motive, subscript  $m$ ). F-ATPase is coupled to inward proton current into  
 606 the negative (neg) compartment,  $J_{mH^{+}neg}$ , to phosphorylate ADP to ATP. The system is defined  
 607 by the boundaries (full black line) and is not a black box, but is analysed as a compartmental  
 608 system. The negative compartment (neg-compartment, enclosed by the dotted line) is the  
 609 matrix space, separated by the mtIM from the positive compartment (pos-compartment).  
 610  $ADP+P_i$  and ATP are the substrate- and product-compartments (scalar ADP and ATP  
 611 compartments, D-comp. and T-comp.), respectively. At steady-state proton turnover,  $J_{\infty H^{+}}$ , and  
 612 ATP turnover,  $J_{\infty P}$ , maintain concentrations constant, when  $J_{mH^{+}\infty} = J_{mH^{+}pos} = J_{mH^{+}neg}$ , and  $J_{P_{\infty}} = J_{P_{\gg}} = J_{P_{\ll}}$ . Modified from Gnaiger (2014).  
 613

614  
 615 ET-pathway control states are obtained in mitochondrial preparations by depletion of  
 616 endogenous substrates and addition to the mitochondrial respiration medium of fuel substrates  
 617 (Figure 2;  $2[H]$  in Figure 3) and specific inhibitors, activating selected mitochondrial catabolic  
 618 pathways,  $k$ , of electron transfer from the oxidation of fuel substrates to reduction of  $O_2$  (Figure  
 619 2A). Coupling control states and pathway control states are complementary, since  
 620 mitochondrial preparations depend on an exogenous supply of pathway-specific fuel substrates  
 621 and oxygen (Gnaiger 2014).  
 622

623 **Coupling:** In mitochondrial electron transfer, vectorial transmembrane proton flux is  
 624 coupled through the redox proton pumps CI, CIII and CIV to the catabolic flux of scalar  
 625 reactions, collectively measured as  $O_2$  flux (Figure 3). Thus mitochondria are elementary  
 626 components of energy transformation. Energy is a conserved quantity and cannot be lost or  
 627 produced in any internal process (First Law of thermodynamics). Open and closed systems can  
 628 gain or lose energy only by external fluxes—by exchange with the environment. Therefore,  
 629 energy can neither be produced by mitochondria, nor is there any internal process without  
 630 energy conservation. Exergy or Gibbs energy (‘free energy’) is the part of energy that can  
 631 potentially be transformed into work under conditions of constant volume and pressure.  
 Coupling is the interaction of an exergonic process (spontaneous, negative exergy change) with

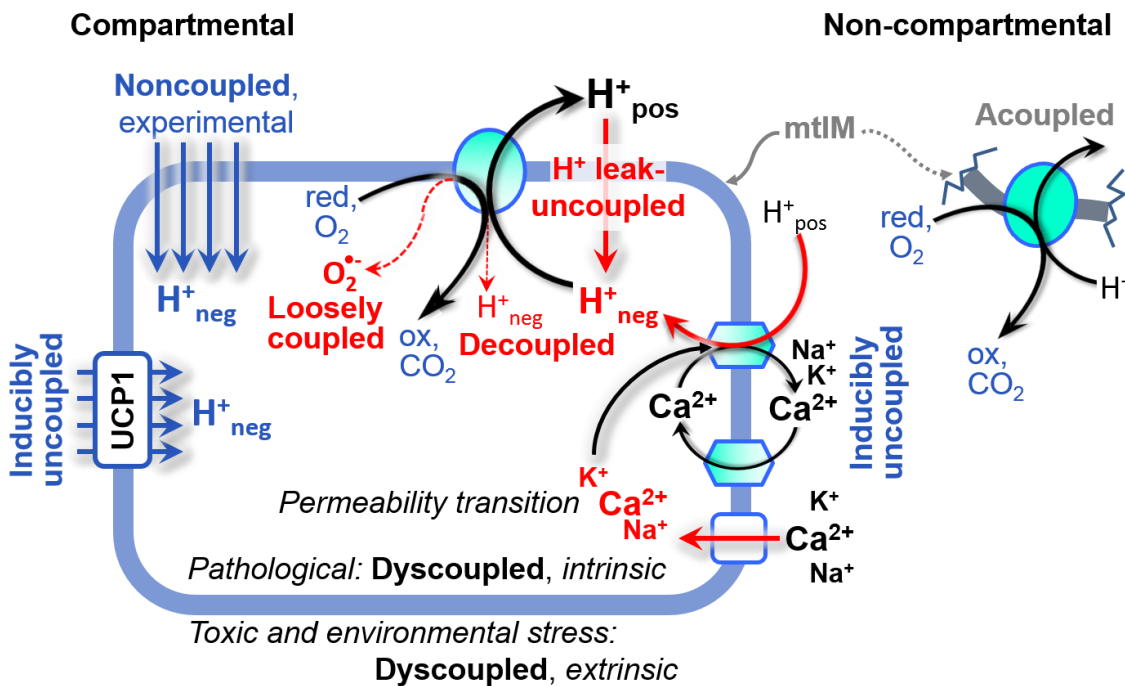
632 an endergonic process (positive exergy change) in energy transformations which conserve part  
 633 of the exergy that would be irreversibly lost or dissipated in an uncoupled process.

634 **Uncoupling:** Uncoupling of mitochondrial respiration is a general term comprising  
 635 diverse mechanisms:

- 636 1. Proton leak across the mtIM from the pos- to the neg-compartment ( $H^+$  leak-  
 637 uncoupled; **Figure 4**).
- 638 2. Cycling of other cations, strongly stimulated by permeability transition; comparable  
 639 to the use of protonophores, cation cycling is experimentally induced by valinomycin  
 640 in the presence of  $K^+$ ;
- 641 3. Decoupling by proton slip in the redox proton pumps when protons are effectively not  
 642 pumped (CI, CIII and CIV) or are not driving phosphorylation (F-ATPase);
- 643 4. Loss of vesicular (compartmental) integrity when electron transfer is uncoupled;
- 644 5. Electron leak in the loosely coupled univalent reduction of  $O_2$  to superoxide ( $O_2^{\bullet-}$ ;  
 645 superoxide anion radical).

646 Differences of terms—uncoupled *vs.* noncoupled—are easily overlooked, although they relate  
 647 to different meanings of uncoupling (**Figure 4** and **Table 2**).

648  
 649



650  
 651  
 652  
 653  
 654  
 655  
 656  
 657  
 658  
 659  
 660  
 661  
 662  
 663  
 664

#### Figure 4. Mechanisms of respiratory uncoupling

An intact mitochondrial inner membrane, mtIM, is required for vectorial, compartmental coupling. ‘Acoupled’ respiration is the consequence of structural disruption with catalytic activity of non-compartmental mitochondrial fragments. Inducibly uncoupled (activation of UCP1) and experimentally noncoupled respiration (titration of protonophores) stimulate respiration to maximum  $O_2$  flux.  $H^+$  leak-uncoupled, decoupled, and loosely coupled respiration are components of intrinsic uncoupling (**Table 2**). Pathological dysfunction may affect all types of uncoupling, including permeability transition, causing intrinsically dyscoupled respiration. Similarly, toxicological and environmental stress factors can cause extrinsically dyscoupled respiration. Reduced fuel substrates, red; oxidized products, ox.

## 665 2.2. Coupling states and respiratory rates

666

667

668 **Respiratory capacities in coupling control states:** To extend the classical nomenclature  
 669 on mitochondrial coupling states (Section 2.3) by a concept-driven terminology that explicitly  
 670 incorporates information on the meaning of respiratory states, the terminology must be general  
 671 and not restricted to any particular experimental protocol or mitochondrial preparation (Gnaiger  
 672 2009). Concept-driven nomenclature aims at mapping the *meaning and concept behind the*  
 673 *words and acronyms onto the forms of words and acronyms* (Miller 1991). The focus of  
 674 concept-driven nomenclature is primarily the conceptual ‘why’, along with clarification of the  
 675 experimental ‘how’. Respiratory capacities delineate, comparable to channel capacity in  
 676 information theory (Schneider 2006), the upper bound of the rate of respiration measured in  
 677 defined coupling control states and electron transfer-pathway (ET-pathway) states (**Figure 5**).

677

678

### 679 **Figure 5. Four-compartment model of oxidative phosphorylation**

680 **model of oxidative phosphorylation**  
 681 Respiratory states (ET, OXPHOS, LEAK; **Table 1**) and  
 682 corresponding rates ( $E$ ,  $P$ ,  $L$ ) are  
 683 connected by the protonmotive force,  $\Delta p$ . (1) ET-capacity,  $E$ , is  
 684 partitioned into (2) dissipative LEAK-respiration,  $L$ , when the  
 685 Gibbs energy change of catabolic  
 686  $O_2$  flux is irreversibly lost, (3) net OXPHOS-capacity,  $P-L$ , with partial conservation of the  
 687 capacity to perform work, and (4) the excess capacity,  $E-P$ . Modified from Gnaiger (2014).

688

689

690

691

692

693

694

695

696

697

698

699

700

701

702

703

704

705

706

707

708

709

710

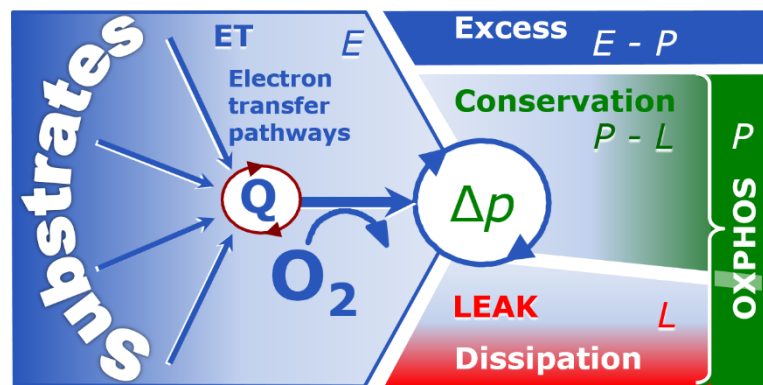
711

712

713

714

715



694 To provide a diagnostic reference for respiratory capacities of core energy metabolism,  
 695 the capacity of *oxidative phosphorylation*, OXPHOS, is measured at kinetically-saturating  
 696 concentrations of ADP and  $P_i$ . The *oxidative* ET-capacity reveals the limitation of OXPHOS-  
 697 capacity mediated by the *phosphorylation*-pathway. The ET- and phosphorylation-pathways  
 698 comprise coupled segments of the OXPHOS-system. ET-capacity is measured as noncoupled  
 699 respiration by application of *external uncouplers*. The contribution of *intrinsically uncoupled*  
 700  $O_2$  consumption is studied by preventing the stimulation of phosphorylation either in the  
 701 absence of ADP or by inhibition of the phosphorylation-pathway. The corresponding states are  
 702 collectively classified as LEAK-states, when  $O_2$  consumption compensates mainly for ion  
 703 leaks, including the proton leak. Defined coupling states are induced by: (1) adding cation  
 704 chelators such as EGTA, binding free  $Ca^{2+}$  and thus limiting cation cycling; (2) adding ADP  
 705 and  $P_i$ ; (3) inhibiting the phosphorylation-pathway; and (4) uncoupler titrations, while  
 706 maintaining a defined ET-pathway state with constant fuel substrates and inhibitors of specific  
 707 branches of the ET-pathway (**Figure 5**).

708 The three coupling states, ET, LEAK and OXPHOS, are shown schematically with the  
 709 corresponding respiratory rates, abbreviated as  $E$ ,  $L$  and  $P$ , respectively (**Figure 5**). We  
 710 distinguish metabolic *pathways* from metabolic *states* and the corresponding metabolic *rates*;  
 711 for example: ET-pathways, ET-states, and ET-capacities,  $E$ , respectively (**Table 1**). The  
 712 protonmotive force is *high* in the OXPHOS-state when it drives phosphorylation, *maximum* in  
 713 the LEAK-state of coupled mitochondria, driven by LEAK-respiration at a minimum back-flux  
 714 of cations to the matrix side, and *very low* in the ET-state when uncouplers short-circuit the  
 715 proton cycle (**Table 1**).

716 **LEAK-state (Figure 6A):**  
 717 The LEAK-state is defined as a  
 718 state of mitochondrial respiration  
 719 when  $O_2$  flux mainly  
 720 compensates for ion leaks in the  
 721 absence of ATP synthesis, at  
 722 kinetically-saturating  
 723 concentrations of  $O_2$ , respiratory  
 724 fuel substrates and  $P_i$ . LEAK-  
 725 respiration is measured to obtain  
 726 an estimate of *intrinsic*  
 727 *uncoupling* without addition of an  
 728 experimental uncoupler: (1) in the  
 729 absence of adenylates, *i.e.*, AMP,  
 730 ADP and ATP; (2) after depletion  
 731 of ADP at a maximum ATP/ADP  
 732 ratio; or (3) after inhibition of the  
 733 phosphorylation-pathway by  
 734 inhibitors of F-ATPase—such as  
 735 oligomycin, or of adenine  
 736 nucleotide translocase—such as  
 737 carboxyatractyloside.  
 738 Adjustment of the nominal  
 739 concentration of these inhibitors  
 740 to the density of biological  
 741 sample applied can minimize or  
 742 avoid inhibitory side-effects  
 743 exerted on ET-capacity or even  
 744 some dyscoupling.

745 • **Proton leak and uncoupled respiration:**

746 The intrinsic proton leak is  
 747 the *uncoupled* leak current  
 748 of protons in which  
 749 protons diffuse across the  
 750 mtIM in the dissipative  
 751 direction of the downhill  
 752 protonmotive force  
 753 without coupling to  
 754 phosphorylation (Figure  
 755 6A). The proton leak flux  
 756 depends non-linearly on  
 757 the protonmotive force  
 758 (Garlid *et al.* 1989;  
 759 Divakaruni and Brand  
 760 2011), it is a temperature-  
 761 dependent property of the  
 762 mtIM and may be enhanced  
 763 due to possible contaminations  
 764 by free fatty acids. Inducible  
 765 uncoupling mediated by  
 766 uncoupling protein 1 (UCP1)  
 is physiologically controlled, *e.g.*,  
 in brown adipose tissue. UCP1  
 is a member of the mitochondrial  
 carrier family that is involved  
 in the translocation of protons  
 across the mtIM (Klingenberg  
 2017).

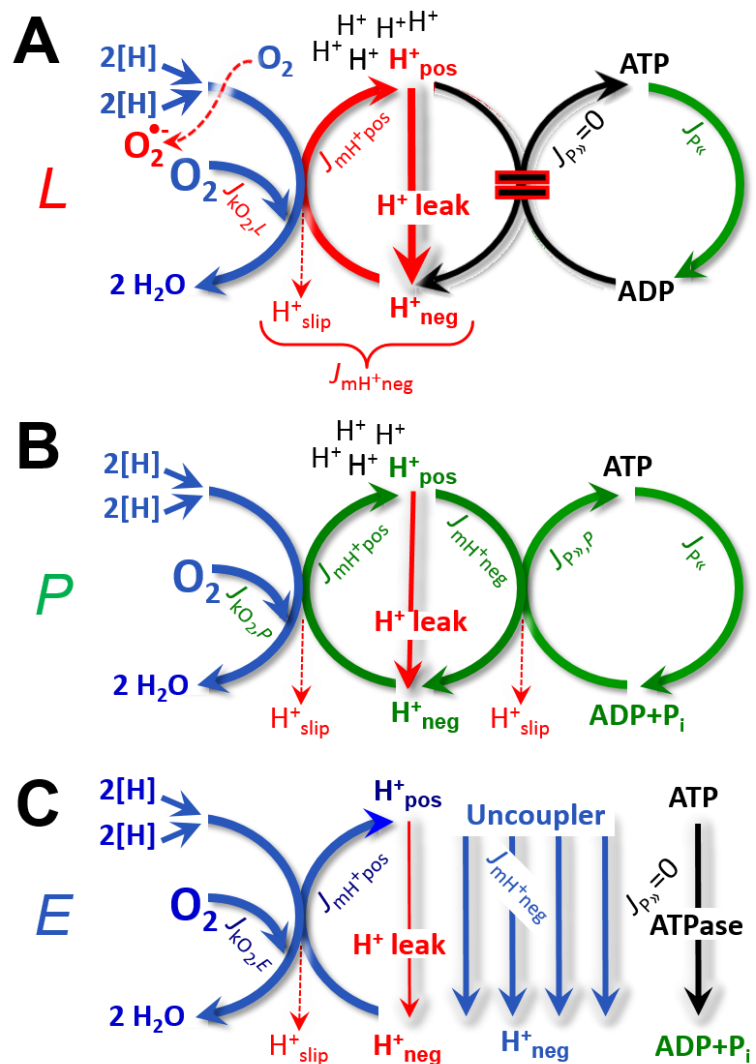


**Figure 6. Respiratory coupling states**

(A) **LEAK-state and rate, L:** Phosphorylation is arrested,  $J_{P\gg} = 0$ , and catabolic  $O_2$  flux,  $J_{kO_2,L}$ , is controlled mainly by the proton leak,  $J_{mH^{+neg},L}$ , at maximum protonmotive force (Figure 4). Extramitochondrial ATP may be hydrolyzed by extramitochondrial ATPases,  $J_{P\ll}$ .

(B) **OXPHOS-state and rate, P:** Phosphorylation,  $J_{P\gg}$ , is stimulated by kinetically-saturating  $[ADP]$  and  $[P_i]$ , and is supported by a high protonmotive force.  $O_2$  flux,  $J_{kO_2,P}$ , is well-coupled at a  $P\gg/O_2$  ratio of  $J_{P\gg,P}/J_{kO_2,P}$ . Extramitochondrial ATPases may recycle ATP,  $J_{P\ll}$ .

(C) **ET-state and rate, E:** Noncoupled respiration,  $J_{kO_2,E}$ , is maximum at optimum exogenous uncoupler concentration and phosphorylation is zero,  $J_{P\gg} = 0$ . The F-ATPase may hydrolyze extramitochondrial ATP. See also Figure 3.



767 Consequently, the short-circuit diminishes the protonmotive force and stimulates electron  
768 transfer to O<sub>2</sub> and heat dissipation without phosphorylation of ADP.

- 769 • **Cation cycling:** There can be other cation contributors to leak current including calcium  
770 and probably magnesium. Calcium influx is balanced by mitochondrial Na<sup>+</sup>/Ca<sup>2+</sup> or  
771 H<sup>+</sup>/Ca<sup>2+</sup> exchange, which is balanced by Na<sup>+</sup>/H<sup>+</sup> or K<sup>+</sup>/H<sup>+</sup> exchanges. This is another  
772 effective uncoupling mechanism different from proton leak (**Table 2**).

773

774 **Table 1. Coupling states and residual oxygen consumption in mitochondrial**  
775 **preparations in relation to respiration- and phosphorylation-flux,  $J_{kO_2}$  and  $J_{P\gg}$ ,**  
776 **and protonmotive force,  $\Delta p$ .** Coupling states are established at kinetically-  
777 saturating concentrations of fuel substrates and O<sub>2</sub>.

State	$J_{kO_2}$	$J_{P\gg}$	$\Delta p$	Inducing factors	Limiting factors
LEAK	$L$ ; low, cation leak-dependent respiration	0	max.	back-flux of cations including proton leak, proton slip	$J_{P\gg} = 0$ : (1) without ADP, $L_N$ ; (2) max. ATP/ADP ratio, $L_T$ ; or (3) inhibition of the phosphorylation-pathway, $L_{Omy}$
OXPHOS	$P$ ; high, ADP-stimulated respiration	max.	high	kinetically-saturating [ADP] and [P <sub>i</sub> ]	$J_{P\gg}$ by phosphorylation-pathway; or $J_{kO_2}$ by ET-capacity
ET	$E$ ; max., noncoupled respiration	0	low	optimal external uncoupler concentration for max. $J_{O_2,E}$	$J_{kO_2}$ by ET-capacity
ROX	$R_{ox}$ ; min., residual O <sub>2</sub> consumption	0	0	$J_{O_2,Rox}$ in non-ET-pathway oxidation reactions	inhibition of all ET-pathways; or absence of fuel substrates

778

- 779 • **Proton slip and decoupled respiration:** Proton slip is the *decoupled* process in which  
780 protons are only partially translocated by a redox proton pump of the ET-pathways and  
781 slip back to the original vesicular compartment. The proton leak is the dominant  
782 contributor to the overall leak current in mammalian mitochondria incubated under  
783 physiological conditions at 37 °C, whereas proton slip is increased at lower experimental  
784 temperature (Canton *et al.* 1995). Proton slip can also happen in association with the F-  
785 ATPase, in which the proton slips downhill across the pump to the matrix without  
786 contributing to ATP synthesis. In each case, proton slip is a property of the proton pump  
787 and increases with the pump turnover rate.

- 788 • **Electron leak and loosely coupled respiration:** Superoxide production by the ETS leads  
789 to a bypass of redox proton pumps and correspondingly lower P<sub>»</sub>/O<sub>2</sub> ratio. This depends  
790 on the actual site of electron leak and the scavenging of hydrogen peroxide by cytochrome  
791 *c*, whereby electrons may re-enter the ETS with proton translocation by CIV.

- 792 • **Loss of compartmental integrity and acoupled respiration:** Electron transfer and  
793 catabolic O<sub>2</sub> flux proceed without compartmental proton translocation in disrupted  
794 mitochondrial fragments. Such fragments form during mitochondrial isolation, and may  
795 not fully fuse to re-establish structurally intact mitochondria. Loss of mtIM integrity,  
796 therefore, is the cause of acoupled respiration, which is a nonvectorial dissipative process  
797 without control by the protonmotive force.

- 798 • **Dyscoupled respiration:** Mitochondrial injuries may lead to *dyscoupling* as a  
 799 pathological or toxicological cause of *uncoupled* respiration. Dyscoupling may involve  
 800 any type of uncoupling mechanism, *e.g.*, opening the permeability transition pore.  
 801 Dyscoupled respiration is distinguished from the experimentally induced *noncoupled*  
 802 respiration in the ET-state (**Table 2**).  
 803  
 804

**Table 2. Terms on respiratory coupling and uncoupling.**

Term	$J_{kO_2}$	$P \gg O_2$	Notes	
acoupled		0	electron transfer in mitochondrial fragments without vectorial proton translocation ( <b>Figure 4</b> )	
intrinsic, no protonophore added	uncoupled	$L$	0	non-phosphorylating LEAK-respiration ( <b>Figure 6A</b> )
	proton leak-uncoupled		0	component of $L$ , $H^+$ diffusion across the mtIM ( <b>Figure 4</b> )
	decoupled		0	component of $L$ , proton slip ( <b>Figure 4</b> )
	loosely coupled		0	component of $L$ , lower coupling due to superoxide formation and bypass of proton pumps by electron leak ( <b>Figure 4</b> )
	dyscoupled		0	pathologically, toxicologically, environmentally increased uncoupling, mitochondrial dysfunction
	inducibly uncoupled		0	by UCP1 or cation ( <i>e.g.</i> , $Ca^{2+}$ ) cycling ( <b>Figure 4</b> )
noncoupled	$E$	0	non-phosphorylating respiration stimulated to maximum flux at optimum exogenous uncoupler concentration ( <b>Figure 6C</b> )	
well-coupled	$P$	high	phosphorylating respiration with an intrinsic LEAK component ( <b>Figure 6B</b> )	
fully coupled	$P - L$	max.	OXPHOS-capacity corrected for LEAK-respiration ( <b>Figure 5</b> )	

805

806

807

808

809

810

811

812

813

814

815

816

817

818

819

820

821

**OXPHOS-state (Figure 6B):** The OXPHOS-state is defined as the respiratory state with kinetically-saturating concentrations of  $O_2$ , respiratory and phosphorylation substrates, and absence of exogenous uncoupler, which provides an estimate of the maximal respiratory capacity in the OXPHOS-state for any given ET-pathway state. Respiratory capacities at kinetically-saturating substrate concentrations provide reference values or upper limits of performance, aiming at the generation of data sets for comparative purposes. Physiological activities and effects of substrate kinetics can be evaluated relative to the OXPHOS-capacity.

As discussed previously, 0.2 mM ADP does not fully saturate flux in isolated mitochondria (Gnaiger 2001; Puchowicz *et al.* 2004); greater ADP concentration is required, particularly in permeabilized muscle fibres and cardiomyocytes, to overcome limitations by intracellular diffusion and by the reduced conductance of the mtOM (Jepihhina *et al.* 2011, Illaste *et al.* 2012, Simson *et al.* 2016), either through interaction with tubulin (Rostovtseva *et al.* 2008) or other intracellular structures (Birkedal *et al.* 2014). In addition, saturating ADP concentrations need to be evaluated under different experimental conditions such as temperature (Lemieux *et al.* 2017) and with different animal models (Blier and Guderley,

1993). In permeabilized muscle fibre bundles of high respiratory capacity, the apparent  $K_m$  for ADP increases up to 0.5 mM (Saks *et al.* 1998), consistent with experimental evidence that >90% saturation is reached only at >5 mM ADP (Pesta and Gnaiger 2012). Similar ADP concentrations are also required for accurate determination of OXPHOS-capacity in human clinical cancer samples and permeabilized cells (Klepinin *et al.* 2016; Koit *et al.* 2017). Whereas 2.5 to 5 mM ADP is sufficient to obtain the actual OXPHOS-capacity in many types of permeabilized tissue and cell preparations, experimental validation is required in each specific case.

**Electron transfer-state (Figure 6C):**  $O_2$  flux determined in the ET-state yields an estimate of ET-capacity. The ET-state is defined as the *noncoupled* state with kinetically-saturating concentrations of  $O_2$ , respiratory substrate and optimum *exogenous* uncoupler concentration for maximum  $O_2$  flux. As a consequence of the nearly collapsed protonmotive force, the driving force is insufficient for phosphorylation, and  $J_{P\gg} = 0$ . The most frequently used uncouplers are carbonyl cyanide *m*-chloro phenyl hydrazone (CCCP), carbonyl cyanide *p*-trifluoromethoxyphenylhydrazone (FCCP), or dinitrophenole (DNP). Stepwise titration of uncouplers stimulates respiration up to or above the level of  $O_2$  consumption rates in the OXPHOS-state, but inhibition of respiration is observed above optimum uncoupler concentrations (Mitchell 2011). Data obtained with a single dose of uncoupler must be evaluated with caution, particularly when a fixed uncoupler concentration is used in studies exploring a treatment or disease that may alter the mitochondrial content or mitochondrial sensitivity to inhibition by uncouplers. The effect on ET-capacity of the reversed function of F-ATPase ( $J_{P\ll}$ ; Figure 6C) can be evaluated in the presence and absence of extramitochondrial ATP.

**ROX state and *Rox*:** Besides the three fundamental coupling states of mitochondrial preparations, the state of residual  $O_2$  consumption, ROX, is relevant to assess respiratory function (Figure 1). ROX is not a coupling state. The rate of residual oxygen consumption, *Rox*, is defined as  $O_2$  consumption due to oxidative reactions measured after inhibition of ET—with rotenone, malonic acid and antimycin A. Cyanide and azide inhibit not only CIV but catalase and several peroxidases involved in *Rox*. However, high concentrations of antimycin A, but not rotenone or cyanide, inhibit peroxisomal acyl-CoA oxidase and D-amino acid oxidase (Vamecq *et al.* 1987). ROX represents a baseline that is used to correct respiration measured in defined coupling states. *Rox*-corrected  $L$ ,  $P$  and  $E$  not only lower the values of total fluxes, but also changes the flux control ratios  $L/P$  and  $L/E$ . *Rox* is not necessarily equivalent to non-mitochondrial reduction of  $O_2$ , considering  $O_2$ -consuming reactions in mitochondria that are not related to ET—such as  $O_2$  consumption in reactions catalyzed by monoamine oxidases (type A and B), monooxygenases (cytochrome P450 monooxygenases), dioxygenase (sulfur dioxygenase and trimethyllysine dioxygenase), and several hydroxylases. Even isolated mitochondrial fractions, especially those obtained from liver, may be contaminated by peroxisomes. This fact makes the exact determination of mitochondrial  $O_2$  consumption and mitochondria-associated generation of reactive oxygen species complicated (Schönfeld *et al.* 2009; Spejger 2016; Figure 2). The dependence of ROX-linked  $O_2$  consumption needs to be studied in detail together with non-ET enzyme activities, availability of specific substrates,  $O_2$  concentration, and electron leakage leading to the formation of reactive oxygen species.

**Quantitative relations:**  $E$  may exceed or be equal to  $P$ .  $E > P$  is observed in many types of mitochondria, varying between species, tissues and cell types (Gnaiger 2009).  $E - P$  is the excess ET-capacity pushing the phosphorylation-flux (Figure 2C) to the limit of its *capacity of utilizing* the protonmotive force. In addition, the magnitude of  $E - P$  depends on the tightness of respiratory coupling or degree of uncoupling, since an increase of  $L$  causes  $P$  to increase towards the limit of  $E$ . The *excess*  $E - P$  capacity,  $E - P$ , therefore, provides a sensitive diagnostic indicator of specific injuries of the phosphorylation-pathway, under conditions when  $E$  remains constant but  $P$  declines relative to controls (Figure 5). Substrate cocktails supporting

873 simultaneous convergent electron transfer to the Q-junction for reconstitution of TCA cycle  
 874 function establish pathway control states with high ET-capacity, and consequently increase the  
 875 sensitivity of the *E-P* assay.

876 *E* cannot theoretically be lower than *P*.  $E < P$  must be discounted as an artefact, which  
 877 may be caused experimentally by: (1) loss of oxidative capacity during the time course of the  
 878 respirometric assay, since *E* is measured subsequently to *P*; (2) using insufficient uncoupler  
 879 concentrations; (3) using high uncoupler concentrations which inhibit ET (Gnaiger 2008); (4)  
 880 high oligomycin concentrations applied for measurement of *L* before titrations of uncoupler,  
 881 when oligomycin exerts an inhibitory effect on *E*. On the other hand, the excess ET-capacity is  
 882 overestimated if non-saturating [ADP] or [P<sub>i</sub>] are used. See State 3 in the next section.

883 The net OXPHOS-capacity is calculated by subtracting *L* from *P* (**Figure 5**). The net  
 884  $P \gg O_2$  equals  $P \gg (P-L)$ , wherein the dissipative LEAK component in the OXPHOS-state may  
 885 be overestimated. This can be avoided by measuring LEAK-respiration in a state when the  
 886 protonmotive force is adjusted to its slightly lower value in the OXPHOS-state—by titration of  
 887 an ET inhibitor (Divakaruni and Brand 2011). Any turnover-dependent components of proton  
 888 leak and slip, however, are underestimated under these conditions (Garlid *et al.* 1993). In  
 889 general, it is inappropriate to use the term *ATP production* or *ATP turnover* for the difference  
 890 of O<sub>2</sub> flux measured in the OXPHOS and LEAK states. *P-L* is the upper limit of OXPHOS-  
 891 capacity that is freely available for ATP production (corrected for LEAK-respiration) and is  
 892 fully coupled to phosphorylation with a maximum mechanistic stoichiometry (**Figure 5**).

893 The rates of LEAK respiration and OXPHOS capacity depend on (1) the tightness of  
 894 coupling under the influence of the respiratory uncoupling mechanisms (**Figure 4**), and (2) the  
 895 coupling stoichiometry, which varies as a function of the substrate type undergoing oxidation  
 896 in ET-pathways with either two or three coupling sites (**Figure 2B**). When cocktails with  
 897 NADH-linked substrates and succinate are used, the relative contribution of ET-pathways with  
 898 three or two coupling sites cannot be controlled experimentally, is difficult to determine, and  
 899 may shift in transitions between LEAK-, OXPHOS- and ET-states (Gnaiger 2014). Under these  
 900 experimental conditions, we cannot separate the tightness of coupling *versus* coupling  
 901 stoichiometry as the mechanisms of respiratory control in the shift of *L/P* ratios. The tightness  
 902 of coupling and fully coupled O<sub>2</sub> flux, *P-L* (**Table 2**), therefore, are obtained from  
 903 measurements of coupling control of LEAK respiration, OXPHOS- and ET-capacities in well  
 904 defined pathway states, using either pyruvate and malate as substrates or the classical succinate  
 905 and rotenone substrate-inhibitor combination (**Figure 2B**).

906

### 907 2.3. Classical terminology for isolated mitochondria

908 ‘When a code is familiar enough, it ceases appearing like a code; one forgets that there  
 909 is a decoding mechanism. The message is identical with its meaning’ (Hofstadter 1979).

910

911 Chance and Williams (1955; 1956) introduced five classical states of mitochondrial  
 912 respiration and cytochrome redox states. **Table 3** shows a protocol with isolated mitochondria  
 913 in a closed respirometric chamber, defining a sequence of respiratory states. States and rates  
 914 are not specifically distinguished in this nomenclature.

915 **State 1** is obtained after addition of isolated mitochondria to air-saturated  
 916 isoosmotic/isotonic respiration medium containing P<sub>i</sub>, but no fuel substrates and no adenylates,  
 917 *i.e.*, AMP, ADP, ATP.

918 **State 2** is induced by addition of a ‘high’ concentration of ADP (typically 100 to 300  
 919 μM), which stimulates respiration transiently on the basis of endogenous fuel substrates and  
 920 phosphorylates only a small portion of the added ADP. State 2 is then obtained at a low  
 921 respiratory activity limited by exhausted endogenous fuel substrate availability (**Table 3**). If  
 922 addition of specific inhibitors of respiratory complexes—such as rotenone—does not cause a  
 923 further decline of O<sub>2</sub> flux, State 2 is equivalent to the ROX state (See below.). If inhibition is

924 observed, undefined endogenous fuel substrates are a confounding factor of pathway control,  
 925 contributing to the effect of subsequently externally added substrates and inhibitors. In contrast  
 926 to the original protocol, an alternative sequence of titration steps is frequently applied, in which  
 927 the alternative 'State 2' has an entirely different meaning, when this second state is induced by  
 928 addition of fuel substrate without ADP or ATP (LEAK-state; in contrast to State 2 defined in  
 929 **Table 1** as a ROX state). Some researchers have called this condition as "pseudostate 4"  
 930 because it has no significant concentrations of adenine nucleotides and hence it is not a near-  
 931 physiological condition, although it should be used for calculating the net OXPHOS-capacity,  
 932 *P-L*.

933  
 934 **Table 3. Metabolic states of mitochondria (Chance and**  
 935 **Williams, 1956; Table V).**  
 936

State	[O <sub>2</sub> ]	ADP level	Substrate level	Respiration rate	Rate-limiting substance
1	>0	low	low	slow	ADP
2	>0	high	~0	slow	substrate
3	>0	high	high	fast	respiratory chain
4	>0	low	high	slow	ADP
5	0	high	high	0	oxygen

937  
 938  
 939 **State 3** is the state stimulated by addition of fuel substrates while the ADP concentration  
 940 is still high (**Table 3**) and supports coupled energy transformation through oxidative  
 941 phosphorylation. 'High ADP' is a concentration of ADP specifically selected to allow the  
 942 measurement of State 3 to State 4 transitions of isolated mitochondria in a closed respirometric  
 943 chamber. Repeated ADP titration re-establishes State 3 at 'high ADP'. Starting at O<sub>2</sub>  
 944 concentrations near air-saturation (193 or 238 μM O<sub>2</sub> at 37 °C or 25 °C and sea level at 1 atm  
 945 or 101.32 kPa, and an oxygen solubility of respiration medium at 0.92 times that of pure water;  
 946 Forstner and Gnaiger 1983), the total ADP concentration added must be low enough (typically  
 947 100 to 300 μM) to allow phosphorylation to ATP at a coupled O<sub>2</sub> flux that does not lead to O<sub>2</sub>  
 948 depletion during the transition to State 4. In contrast, kinetically-saturating ADP concentrations  
 949 usually are 10-fold higher than 'high ADP', *e.g.*, 2.5 mM in isolated mitochondria. The  
 950 abbreviation State 3u is occasionally used in bioenergetics, to indicate the state of respiration  
 951 after titration of an uncoupler, without sufficient emphasis on the fundamental difference  
 952 between OXPHOS-capacity (*well-coupled* with an *endogenous* uncoupled component) and ET-  
 953 capacity (*noncoupled*).

954 **State 4** is a LEAK-state that is obtained only if the mitochondrial preparation is intact  
 955 and well-coupled. Depletion of ADP by phosphorylation to ATP causes a decline of O<sub>2</sub> flux in  
 956 the transition from State 3 to State 4. Under the conditions of State 4, a maximum protonmotive  
 957 force and high ATP/ADP ratio are maintained. The gradual decline of  $Y_{P_{\gg}/O_2}$  towards  
 958 diminishing [ADP] at State 4 must be taken into account for calculation of  $P_{\gg}/O_2$  ratios (Gnaiger  
 959 2001). State 4 respiration,  $L_T$  (**Table 1**), reflects intrinsic proton leak and ATP hydrolysis  
 960 activity. O<sub>2</sub> flux in State 4 is an overestimation of LEAK-respiration if the contaminating ATP  
 961 hydrolysis activity recycles some ATP to ADP,  $J_{P_{\ll}}$ , which stimulates respiration coupled to  
 962 phosphorylation,  $J_{P_{\gg}} > 0$ . Some degree of mechanical disruption and loss of mitochondrial  
 963 integrity allows the exposed mitochondrial F-ATPases to hydrolyze the ATP synthesized by  
 964 the fraction of coupled mitochondria. This can be tested by inhibition of the phosphorylation-  
 965 pathway using oligomycin, ensuring that  $J_{P_{\gg}} = 0$  (State 4o). On the other hand, the state 4  
 966 respiration reached after exhaustion of added ADP is a more physiological condition (*i.e.*,  
 967 presence of ATP, ADP and even AMP). Sequential ADP titrations re-establish State 3, followed

968 by State 3 to State 4 transitions while sufficient O<sub>2</sub> is available. Anoxia may be reached,  
969 however, before exhaustion of ADP (State 5).

970 **State 5** is the state after exhaustion of O<sub>2</sub> in a closed respirometric chamber. Diffusion of  
971 O<sub>2</sub> from the surroundings into the aqueous solution may be a confounding factor preventing  
972 complete anoxia (Gnaiger 2001). Chance and Williams (1955) provide an alternative definition  
973 of State 5, which gives it the different meaning of ROX versus anoxia: ‘State 5 may be obtained  
974 by antimycin A treatment or by anaerobiosis’.

975 In **Table 3**, only States 3 and 4 are coupling control states, with the restriction that rates  
976 in State 3 may be limited kinetically by non-saturating ADP concentrations.

977

978

### 979 3. What is a rate?

980

981 A rate may be considered as the numerator and normalization as the complementary  
982 denominator, which are tightly linked in reporting the measurements in a format commensurate  
983 with the requirements of a database. Application of common and defined units is required for  
984 direct transfer of reported results into a database. The second [s] is the SI unit for the base  
985 quantity *time*. It is also the standard time-unit used in solution chemical kinetics.

986 The term *rate* is not adequately defined to be useful for reporting data. The inconsistency  
987 of the meanings of rate becomes apparent when considering Galileo Galilei’s famous principle,  
988 that ‘bodies of different weight all fall at the same rate (have a constant acceleration)’  
989 (Coopersmith 2010). A rate may be an extensive quantity, which is a *flow*, *I*, when expressed  
990 per object (per number of cells or organisms) or per chamber (per system). ‘System’ is defined  
991 as the open or closed chamber of the measuring device. A rate is a *flux*, *J*, when expressed as a  
992 size-specific quantity (**Figure 7A; Box 2**).

993

994 • **Extensive quantities:** An extensive quantity increases proportionally with system  
995 size. For example, mass and volume are extensive quantities. Flow is an extensive  
996 quantity. The magnitude of an extensive quantity is completely additive for non-  
997 interacting subsystems. The magnitude of these quantities depends on the extent or  
998 size of the system (Cohen *et al.* 2008).

999 • **Size-specific quantities:** ‘The adjective *specific* before the name of an extensive  
1000 quantity is often used to mean *divided by mass*’ (Cohen *et al.* 2008). In this system-  
1001 paradigm, mass-specific flux is flow divided by mass of the *system* (the total mass of  
1002 everything within the measuring chamber or reactor). Rates are frequently expressed  
1003 as volume-specific flux. A mass-specific or volume-specific quantity is independent  
1004 of the extent of non-interacting homogenous subsystems. Tissue-specific quantities  
1005 (related to the *sample* in contrast to the *system*) are of fundamental interest in the field  
1006 of comparative mitochondrial physiology, where *specific* refers to the *type of the*  
1007 *sample* rather than *mass of the system*. The term *specific*, therefore, must be clarified;  
1008 *sample-specific*, *e.g.*, muscle mass-specific normalization, is distinguished from  
1009 *system-specific* quantities (mass or volume; **Figure 7**).

1010 • **Intensive quantities:** In contrast to size-specific properties, forces are *intensive*  
1011 quantities defined as the change of an extensive quantity per advancement of an  
1012 energy transformation (Gnaiger 1993b).

1013

1014  $N_X$  and  $m_X$  indicate the number format and mass format, respectively, for expressing the  
1015 quantity of a sample *X*. When different formats are indicated in symbols of derived quantities,  
1016 the format ( $\underline{N}$ ,  $\underline{m}$ ) is shown as a subscript (*underlined italic*), as in  $I_{O_2/\underline{N}X}$  and  $J_{O_2/\underline{m}X}$ . Oxygen flow  
1017 and flux are expressed in the molar format,  $n_{O_2}$  [mol], but in the volume format,  $V_{O_2}$  [m<sup>3</sup>] in

1018 ergometry. For mass-specific flux these formats can be distinguished as  $J_{\underline{m}O_2/\underline{m}X}$  and  $J_{\underline{V}O_2/\underline{m}X}$ ,  
 1019 respectively. Further examples are given in **Figure 7** and **Table 4**.

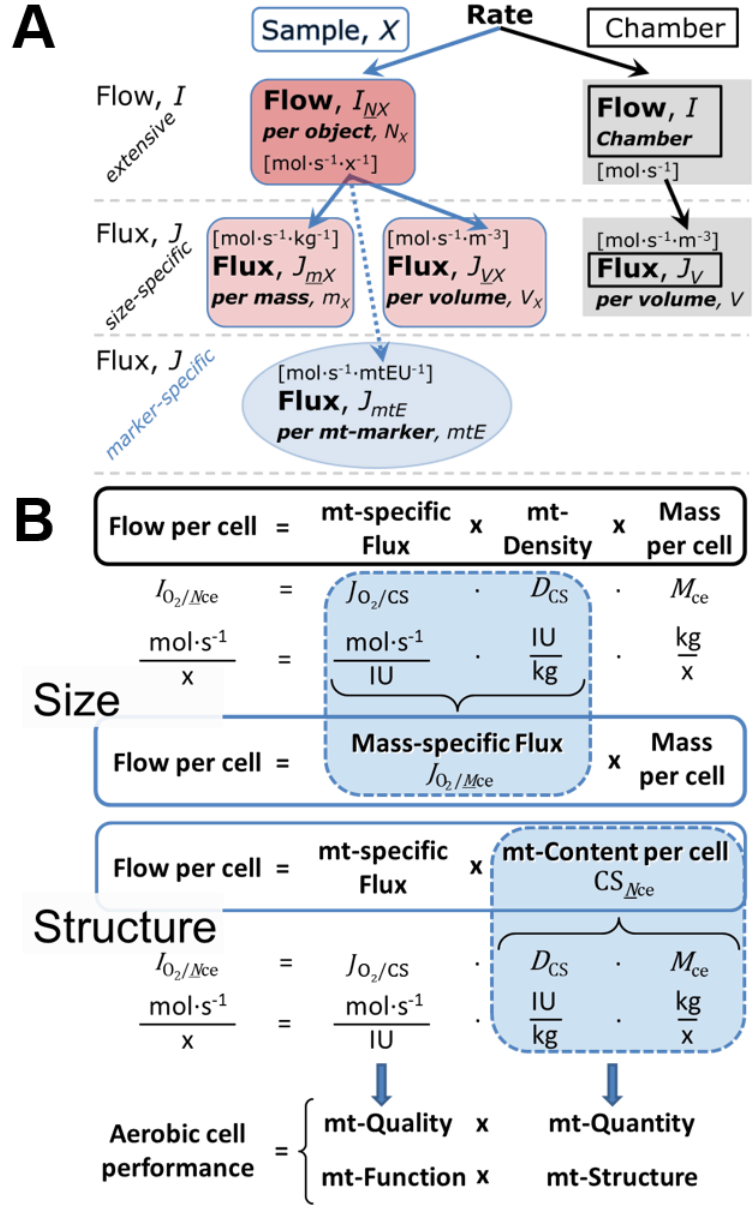
1020  
1021

1022 **Figure 7. Flow and flux, and**  
 1023 **normalization in structure-**  
 1024 **function analysis**

1025 (A) When expressing metabolic  
 1026 ‘rate’ measured in a chamber, a  
 1027 fundamental distinction is made  
 1028 between relating the rate to the  
 1029 experimental sample (left) or  
 1030 chamber (right). The different  
 1031 meanings of rate need to be  
 1032 specified by the chosen  
 1033 normalization. Left: Results are  
 1034 expressed as mass-specific *flux*,  
 1035  $J_{mX}$ , per mg protein, dry or wet  
 1036 weight (mass). Cell volume,  $V_{ce}$ ,  
 1037 may be used for normalization  
 1038 (volume-specific flux,  $J_{Vce}$ ).  
 1039 Right: Flow per chamber,  $I$ , or  
 1040 flux per chamber volume,  $J_V$ , are  
 1041 merely reported for  
 1042 methodological reasons.

1043 (B)  $O_2$  flow per cell,  $I_{O_2/Nce}$ , is the  
 1044 product of mitochondria-specific  
 1045 flux, mt-density and mass per  
 1046 cell. Unstructured analysis:  
 1047 performance is the product of  
 1048 mass-specific flux,  $J_{O_2/MX}$   
 1049 [ $\text{mol}\cdot\text{s}^{-1}\cdot\text{kg}^{-1}$ ], and *size* (mass per  
 1050 cell). Structured analysis:  
 1051 performance is the product of  
 1052 mitochondrial *function* (mt-  
 1053 specific flux) and *structure* (mt-  
 1054 content). Modified from Gnaiger  
 1055 (2014). For further details see  
 1056 **Table 4**.

1057  
1058



1059 **Box 2: Metabolic flows and fluxes: vectoral, vectorial, and scalar**  
 1060

1061 In a generalization of electrical terms, flow as an extensive quantity ( $I$ ; per system) is  
 1062 distinguished from flux as a size-specific quantity ( $J$ ; per system size). *Flows*,  $I_{tr}$ , are defined  
 1063 for all transformations as extensive quantities. Electric charge per unit time is electric flow or  
 1064 current,  $I_{el} = dQ_{el}\cdot dt^{-1}$  [ $A \equiv C\cdot s^{-1}$ ]. When dividing  $I_{el}$  by size of the system (cross-sectional area  
 1065 of a ‘wire’), we obtain flux as a size-specific quantity, which is the current density (surface-  
 1066 density of flow) perpendicular to the direction of flux,  $J_{el} = I_{el}\cdot A^{-1}$  [ $A\cdot m^{-2}$ ] (Cohen et al. 2008).  
 1067 Fluxes with *spatial* geometric direction and magnitude are *vectors*. Vector and scalar *fluxes* are  
 1068 related to flows as  $J_{tr} = I_{tr}\cdot A^{-1}$  [ $\text{mol}\cdot\text{s}^{-1}\cdot\text{m}^{-2}$ ] and  $J_{tr} = I_{tr}\cdot V^{-1}$  [ $\text{mol}\cdot\text{s}^{-1}\cdot\text{m}^{-3}$ ], expressing flux as an  
 1069 area-specific vector or volume-specific vectorial or scalar quantity, respectively (Gnaiger

1070 1993b). We use the metre–kilogram–second–ampere (MKSA) international system of units (*SI*)  
 1071 for general cases ([m], [kg], [s] and [A]), with decimal *SI* prefixes for specific applications  
 1072 (**Table 4**).

1073 We suggest to define: (1) *vectorial* fluxes, which are translocations as functions of  
 1074 *gradients* with direction in geometric space in continuous systems; (2) *vectorial* fluxes, which  
 1075 describe translocations in discontinuous systems and are restricted to information on  
 1076 *compartmental differences* (**Figure 3**, transmembrane proton flux); and (3) *scalar* fluxes, which  
 1077 are transformations in a *homogenous* system (**Figure 3**, catabolic O<sub>2</sub> flux,  $J_{kO_2}$ ).

1078 Vectorial transmembrane proton fluxes,  $J_{mH^{+pos}}$  and  $J_{mH^{+neg}}$ , are analyzed in a  
 1079 heterogenous compartmental system as a quantity with *directional* but not *spatial* information.  
 1080 Translocation of protons across the mtIM has a defined direction, either from the negative  
 1081 compartment (matrix space; negative, neg–compartment) to the positive compartment (inter-  
 1082 membrane space; positive, pos–compartment) or *vice versa* (**Figure 3**). The arrows defining  
 1083 the direction of the translocation between the two vesicular compartments may point upwards  
 1084 or downwards, right or left, without any implication that these are actual directions in space.  
 1085 The pos–compartment is neither above nor below the neg–compartment in a spatial sense, but  
 1086 can be visualized arbitrarily in a figure in the upper position (**Figure 3**). In general, the  
 1087 *compartmental direction* of vectorial translocation from the neg–compartment to the pos–  
 1088 compartment is defined by assigning the initial and final state as *ergodynamic compartments*,  
 1089  $H^{+}_{neg} \rightarrow H^{+}_{pos}$  or  $0 = -1 H^{+}_{neg} + 1 H^{+}_{pos}$ , related to work (erg = work) that must be performed to  
 1090 lift the proton from a lower to a higher electrochemical potential or from the lower to the higher  
 1091 ergodynamic compartment (Gnaiger 1993b).

1092 In analogy to *vectorial* translocation, the direction of a *scalar* chemical reaction,  $A \rightarrow B$   
 1093 or  $0 = -1 A + 1 B$ , is defined by assigning substrates and products, A and B, as ergodynamic  
 1094 compartments. O<sub>2</sub> is defined as a substrate in respiratory O<sub>2</sub> consumption (electron acceptor),  
 1095 which together with the fuel substrates (electron donors) comprises the substrate compartment  
 1096 of the catabolic reaction. Volume-specific scalar O<sub>2</sub> flux is coupled to vectorial translocation,  
 1097 yielding the  $H^{+}_{pos}/O_2$  ratio (**Figure 2B**).

---

1098  
 1099

#### 1100 4. Normalization of rate per sample

1101

1102 The challenges of measuring mitochondrial respiratory flux are matched by those of  
 1103 normalization. Normalization (**Table 4**) is guided by physicochemical principles,  
 1104 methodological considerations, and conceptual strategies (**Figure 7**).

1105

##### 1106 4.1. Flow: per object

1107

1108 **Number concentration,  $C_{NX}$ :** Normalization per sample concentration is routinely  
 1109 required to report respiratory data.  $C_{NX}$  is the experimental *number concentration* of sample X.  
 1110 In the case of animals, e.g., nematodes,  $C_{NX} = N_X/V [x \cdot L^{-1}]$ , where  $N_X$  is the number of organisms  
 1111 in the chamber. Similarly, the number of cells per chamber volume is the number concentration  
 1112 of permeabilized or intact cells  $C_{N_{ce}} = N_{ce}/V [x \cdot L^{-1}]$ , where  $N_{ce}$  is the number of cells in the  
 1113 chamber (**Table 4**).

1114 **Flow per object,  $I_{O_2/N_{ce}}$ :** O<sub>2</sub> flow per cell is calculated from volume-specific O<sub>2</sub> flux,  $J_{V,O_2}$   
 1115 [nmol·s<sup>-1</sup>·L<sup>-1</sup>] (per  $V$  of the measurement chamber [L]), divided by the number concentration of  
 1116 cells. The total cell count is the sum of viable and dead cells,  $N_{ce} = N_{vce} + N_{dce}$  (**Table 5**). The  
 1117 cell viability index,  $VI = N_{vce}/N_{ce}$ , is the ratio of viable cells ( $N_{vce}$ ; before experimental  
 1118 permeabilization) per total cell count. After experimental permeabilization, all cells are  
 1119 permeabilized,  $N_{pce} = N_{ce}$ . The cell viability index can be used to normalize respiration for the  
 1120 number of cells that have been viable before experimental permeabilization,  $I_{O_2/N_{vce}} = I_{O_2/N_{ce}}/VI$ ,



1121 considering that mitochondrial respiratory dysfunction in dead cells should be eliminated as a  
 1122 confounding factor.

1123

1124 **Table 4. Sample concentrations and normalization of flux.**

1125

Expression	Symbol	Definition	Unit	Notes
<b>Sample</b>				
identity of sample	$X$	object: cell, tissue, animal, patient		
number of sample entities $X$	$N_X$	number of objects	x	1
mass of sample $X$	$m_X$		kg	2
mass of object $X$	$M_X$	$M_X = m_X \cdot N_X^{-1}$	$\text{kg} \cdot \text{x}^{-1}$	2
<b>Mitochondria</b>				
Mitochondria	Mt	$X = \text{mt}$		
amount of mt-elementary components	$mtE$	quantity of mt-marker	mtEU	
<b>Concentrations</b>				
object number concentration	$C_{NX}$	$C_{NX} = N_X \cdot V^{-1}$	$\text{x} \cdot \text{m}^{-3}$	3
sample mass concentration	$C_{mX}$	$C_{mX} = m_X \cdot V^{-1}$	$\text{kg} \cdot \text{m}^{-3}$	
mitochondrial concentration	$C_{mtE}$	$C_{mtE} = mtE \cdot V^{-1}$	$\text{mtEU} \cdot \text{m}^{-3}$	4
specific mitochondrial density	$D_{mtE}$	$D_{mtE} = mtE \cdot m_X^{-1}$	$\text{mtEU} \cdot \text{kg}^{-1}$	5
mitochondrial content, $mtE$ per object $X$	$mtE_{NX}$	$mtE_{NX} = mtE \cdot N_X^{-1}$	$\text{mtEU} \cdot \text{x}^{-1}$	6
<b>O<sub>2</sub> flow and flux</b>				
flow, system	$I_{O_2}$	internal flow	$\text{mol} \cdot \text{s}^{-1}$	7
volume-specific flux	$J_{V,O_2}$	$J_{V,O_2} = I_{O_2} \cdot V^{-1}$	$\text{mol} \cdot \text{s}^{-1} \cdot \text{m}^{-3}$	8
flow per object $X$	$I_{O_2/NX}$	$I_{O_2/NX} = J_{V,O_2} \cdot C_{NX}^{-1}$	$\text{mol} \cdot \text{s}^{-1} \cdot \text{x}^{-1}$	9
mass-specific flux	$J_{O_2/mX}$	$J_{O_2/mX} = J_{V,O_2} \cdot C_{mX}^{-1}$	$\text{mol} \cdot \text{s}^{-1} \cdot \text{kg}^{-1}$	10
mt-marker-specific flux	$J_{O_2/mtE}$	$J_{O_2/mtE} = J_{V,O_2} \cdot C_{mtE}^{-1}$	$\text{mol} \cdot \text{s}^{-1} \cdot \text{mtEU}^{-1}$	11

1126 1 The unit x for a number is not used by IUPAC. To avoid confusion, the units [ $\text{kg} \cdot \text{x}^{-1}$ ] and [kg]  
 1127 distinguish the mass per object from the mass of a sample that may contain any number of objects.  
 1128 Similarly, the units for flow per system *versus* flow per object are [ $\text{mol} \cdot \text{s}^{-1}$ ] (Note 8) and [ $\text{mol} \cdot \text{s}^{-1} \cdot \text{x}^{-1}$ ]  
 1129 (Note 10).

1130 2 Units are given in the MKSA system (**Box 2**). The *SI* prefix k is used for the *SI* base unit of mass (kg  
 1131 = 1,000 g). In praxis, various *SI* prefixes are used for convenience, to make numbers easily readable,  
 1132 e.g., 1 mg tissue, cell or mitochondrial mass instead of 0.000001 kg.

1133 3 In case of cells (sample  $X = \text{cells}$ ), the object number concentration is  $C_{N_{ce}} = N_{ce} \cdot V^{-1}$ , and volume  
 1134 may be expressed in [ $\text{dm}^3 \equiv \text{L}$ ] or [ $\text{cm}^3 = \text{mL}$ ]. See **Table 5** for different object types.

1135 4 mt-concentration is an experimental variable, dependent on sample concentration: (1)  $C_{mtE} = mtE \cdot V^{-1}$ ;  
 1136 (2)  $C_{mtE} = mtE_X \cdot C_{NX}$ ; (3)  $C_{mtE} = C_{mX} \cdot D_{mtE}$ .

1137 5 If the amount of mitochondria,  $mtE$ , is expressed as mitochondrial mass, then  $D_{mtE}$  is the mass  
 1138 fraction of mitochondria in the sample. If  $mtE$  is expressed as mitochondrial volume,  $V_{mt}$ , and the  
 1139 mass of sample,  $m_X$ , is replaced by volume of sample,  $V_X$ , then  $D_{mtE}$  is the volume fraction of  
 1140 mitochondria in the sample.

1141 6  $mtE_{NX} = mtE \cdot N_X^{-1} = C_{mtE} \cdot C_{NX}^{-1}$ .

1142 7 O<sub>2</sub> can be replaced by other chemicals B to study different reactions, e.g., ATP, H<sub>2</sub>O<sub>2</sub>, or vesicular  
 1143 compartmental translocations, e.g., Ca<sup>2+</sup>.

1144 8  $I_{O_2}$  and  $V$  are defined per instrument chamber as a system of constant volume (and constant  
 1145 temperature), which may be closed or open.  $I_{O_2}$  is abbreviated for  $I_{rO_2}$ , i.e., the metabolic or internal  
 1146 O<sub>2</sub> flow of the chemical reaction r in which O<sub>2</sub> is consumed, hence the negative stoichiometric  
 1147 number,  $\nu_{O_2} = -1$ .  $I_{rO_2} = d_r n_{O_2} / dt \cdot \nu_{O_2}^{-1}$ . If r includes all chemical reactions in which O<sub>2</sub> participates, then

- 1148  $d_r n_{O_2} = dn_{O_2} - d_e n_{O_2}$ , where  $dn_{O_2}$  is the change in the amount of  $O_2$  in the instrument chamber and  $d_e n_{O_2}$   
 1149 is the amount of  $O_2$  added externally to the system. At steady state, by definition  $dn_{O_2} = 0$ , hence  $d_r n_{O_2}$   
 1150  $= -d_e n_{O_2}$ .
- 1151 9  $J_{V,O_2}$  is an experimental variable, expressed per volume of the instrument chamber.
- 1152 10  $I_{O_2/NX}$  is a physiological variable, depending on the size of entity  $X$ .
- 1153 11 There are many ways to normalize for a mitochondrial marker, that are used in different experimental  
 1154 approaches: (1)  $J_{O_2/mtE} = J_{V,O_2} \cdot C_{mtE}^{-1}$ ; (2)  $J_{O_2/mtE} = J_{V,O_2} \cdot C_{mX}^{-1} \cdot D_{mtE}^{-1} = J_{O_2/mX} \cdot D_{mtE}^{-1}$ ; (3)  $J_{O_2/mtE} =$   
 1155  $J_{V,O_2} \cdot C_{NX}^{-1} \cdot mtE_{NX}^{-1} = I_{O_2/NX} \cdot mtE_{NX}^{-1}$ ; (4)  $J_{O_2/mtE} = I_{O_2} \cdot mtE^{-1}$ . The mt-elementary unit [mtEU] varies depending  
 1156 on the mt-marker.
- 1157  
 1158  
 1159 **Table 5. Sample types, X, abbreviations, and quantification.**

Identity of sample	$X$	$N_X$	Mass <sup>a</sup>	Volume	mt-Marker
mitochondrial preparation		[x]	[kg]	[m <sup>3</sup> ]	[mtEU]
isolated mitochondria	imt		$m_{mt}$	$V_{mt}$	$mtE$
tissue homogenate	thom		$m_{thom}$		$mtE_{thom}$
permeabilized tissue	pti		$m_{pti}$		$mtE_{pti}$
permeabilized fibre	pfi		$m_{pfi}$		$mtE_{pfi}$
permeabilized cell	pce	$N_{pce}$	$M_{pce}$	$V_{pce}$	$mtE_{pce}$
cells <sup>b</sup>	ce	$N_{ce}$	$M_{ce}$	$V_{ce}$	$mtE_{ce}$
intact cell, viable cell	vce	$N_{vce}$	$M_{vce}$	$V_{vce}$	
dead cell	dce	$N_{dce}$	$M_{dce}$	$V_{dce}$	
organism	org	$N_{org}$	$M_{org}$	$V_{org}$	

1160 <sup>a</sup> Instead of mass, the wet weight or dry weight is frequently stated,  $W_w$  or  $W_d$ .  
 1161  $m_X$  is mass of the sample [kg],  $M_X$  is mass of the object [kg·x<sup>-1</sup>] (Table 4).

1162 <sup>b</sup> Total cell count,  $N_{ce} = N_{vce} + N_{dce}$

1163

1164 The complexity changes when the sample is a whole organism studied as an experimental  
 1165 model. The scaling law in respiratory physiology reveals a strong interaction between  $O_2$  flow  
 1166 and individual body mass, since *basal* metabolic rate (flow) does not increase linearly with  
 1167 body mass, whereas *maximum* mass-specific  $O_2$  flux,  $\dot{V}_{O_2max}$  or  $\dot{V}_{O_2peak}$ , is approximately  
 1168 constant across a large range of individual body mass (Weibel and Hoppeler 2005), with  
 1169 individuals, breeds, and species deviating substantially from this relationship.  $\dot{V}_{O_2peak}$  of human  
 1170 endurance athletes is 60 to 80 mL  $O_2 \cdot \text{min}^{-1} \cdot \text{kg}^{-1}$  body mass, converted to  $J_{O_2peak/Morg}$  of 45 to 60  
 1171 nmol·s<sup>-1</sup>·g<sup>-1</sup> (Gnaiger 2014; Table 6).

1172

#### 1173 4.2. Size-specific flux: per sample size

1174

1175 **Sample concentration,  $C_{mX}$ :** Considering permeabilized tissue, homogenate or cells as  
 1176 the sample,  $X$ , the sample mass is  $m_X$  [mg], which is frequently measured as wet or dry weight,  
 1177  $W_w$  or  $W_d$  [mg], respectively, or as amount of protein,  $m_{Protein}$ . The sample concentration is the  
 1178 mass of the subsample per volume of the measurement chamber,  $C_{mX} = m_X/V$  [g·L<sup>-1</sup> = mg·mL<sup>-1</sup>].  
 1179  $X$  is the type of sample—isolated mitochondria, tissue homogenate, permeabilized fibres or  
 1180 cells (Table 5).

1181 **Size-specific flux:** Cellular  $O_2$  flow can be compared between cells of identical size. To  
 1182 take into account changes and differences in cell size, normalization is required to obtain cell  
 1183 size-specific or mitochondrial marker-specific  $O_2$  flux (Renner *et al.* 2003).

- 1184 • **Mass-specific flux,  $J_{O_2/mX}$  [mol·s<sup>-1</sup>·kg<sup>-3</sup>]:** Mass-specific flux is obtained by expressing  
 1185 respiration per mass of sample,  $m_X$  [mg]. Flow per cell is divided by mass per cell,

1186  $J_{O_2/mce} = I_{O_2/Nce}/M_{Nce}$ . Or chamber volume-specific flux,  $J_{V,O_2}$ , is divided by mass  
 1187 concentration of  $X$  in the chamber,  $J_{O_2/mX} = J_{V,O_2}/C_{mX}$ .

1188 • **Cell volume-specific flux,  $J_{O_2/VX}$  [ $\text{mol}\cdot\text{s}^{-1}\cdot\text{m}^{-3}$ ]**: Sample volume-specific flux is  
 1189 obtained by expressing respiration per volume of sample. For example, in the case of  
 1190 using cells as sample will be the volume of cells added to the chamber (**Figure 7**).  
 1191

1192 If size-specific  $O_2$  flux is constant and independent of sample size, then there is no  
 1193 interaction between the subsystems. For example, a 1.5 mg and a 3.0 mg muscle sample respires  
 1194 at identical mass-specific flux. Mass-specific  $O_2$  flux, however, may change with the mass of a  
 1195 tissue sample, cells or isolated mitochondria in the measuring chamber, in which the nature of  
 1196 the interaction becomes an issue. Therefore, cell density must be optimized, particularly in  
 1197 experiments carried out in wells, considering the confluency of the cell monolayer or clumps  
 1198 of cells (Salabei *et al.* 2014).  
 1199

#### 1200 4.3. Marker-specific flux: per mitochondrial content

1201  
 1202 Tissues can contain multiple cell populations that may have distinct mitochondrial  
 1203 subtypes. Mitochondria undergo dynamic fission and fusion cycles, and can exist in multiple  
 1204 stages and sizes that may be altered by a range of factors. The isolation of mitochondria (often  
 1205 achieved through differential centrifugation) can therefore yield a subsample of the  
 1206 mitochondrial types present in a tissue, depending on the isolation protocols utilized (*e.g.*,  
 1207 centrifugation speed). This possible bias should be taken into account when planning  
 1208 experiments using isolated mitochondria. Different sizes of mitochondria are enriched at  
 1209 specific centrifugation speeds, which can be used strategically for isolation of mitochondrial  
 1210 subpopulations.

1211 Part of the mitochondrial content of a tissue is lost during preparation of isolated  
 1212 mitochondria. The fraction of isolated mitochondria obtained from a tissue sample is expressed  
 1213 as mitochondrial recovery. At a high mitochondrial recovery the fraction of isolated  
 1214 mitochondria is more representative of the total mitochondrial population than in preparations  
 1215 characterized by low recovery. Determination of the mitochondrial recovery and yield is based  
 1216 on measurement of the concentration of a mitochondrial marker in the stock of isolated  
 1217 mitochondria,  $C_{mtE,stock}$ , and crude tissue homogenate,  $C_{mtE,thom}$ , which simultaneously provides  
 1218 information on the specific mitochondrial density in the sample,  $D_{mtE}$  (**Table 4**).  
 1219

1220 Normalization is a problematic subject; it is essential to consider the question of the study.  
 1221 If the study aims at comparing tissue performance—such as the effects of a treatment on a  
 1222 specific tissue, then normalization for tissue mass or protein content is appropriate. However,  
 1223 if the aim is to find differences on mitochondrial function independent of mitochondrial density  
 1224 (**Table 4**), then normalization to a mitochondrial marker is imperative (**Figure 7**). One cannot  
 1225 assume that quantitative changes in various markers—such as mitochondrial proteins—  
 1226 necessarily occur in parallel with one another. It should be established that the marker chosen  
 1227 is not selectively altered by the performed treatment. In conclusion, the normalization must  
 1228 reflect the question under investigation to reach a satisfying answer. On the other hand, the goal  
 1229 of comparing results across projects and institutions requires standardization on normalization  
 for entry into a databank.

1230 **Mitochondrial concentration,  $C_{mtE}$ , and mitochondrial markers:** Mitochondrial  
 1231 organelles comprise a dynamic cellular reticulum in various states of fusion and fission. Hence,  
 1232 the definition of an "amount" of mitochondria is often misconceived: mitochondria cannot be  
 1233 counted reliably as a number of occurring elementary components. Therefore, quantification of  
 1234 the "amount" of mitochondria depends on the measurement of chosen mitochondrial markers.  
 1235 'Mitochondria are the structural and functional elementary units of cell respiration' (Gnaiger  
 1236 2014). The quantity of a mitochondrial marker can reflect the amount of *mitochondrial*

1237 *elementary components, mtE*, expressed in various mitochondrial elementary units [mtEU]  
 1238 specific for each measured mt-marker (**Table 4**). However, since mitochondrial quality may  
 1239 change in response to stimuli—particularly in mitochondrial dysfunction (Campos *et al.* 2017)  
 1240 and after exercise training (Pesta *et al.* 2011) and during aging (Daum *et al.* 2013)—some  
 1241 markers can vary while others are unchanged: (1) Mitochondrial volume and membrane area  
 1242 are structural markers, whereas mitochondrial protein mass is frequently used as a marker for  
 1243 isolated mitochondria. (2) Molecular and enzymatic mitochondrial markers (amounts or  
 1244 activities) can be selected as matrix markers, *e.g.*, citrate synthase activity, mtDNA; mtIM-  
 1245 markers, *e.g.*, cytochrome *c* oxidase activity, *aa3* content, cardiolipin, or mtOM-markers, *e.g.*,  
 1246 the voltage-dependent anion channel (VDAC), TOM20. (3) Extending the measurement of  
 1247 mitochondrial marker enzyme activity to mitochondrial pathway capacity, ET- or OXPHOS-  
 1248 capacity can be considered as an integrative functional mitochondrial marker.

1249 Depending on the type of mitochondrial marker, the mitochondrial elementary  
 1250 component, *mtE*, is expressed in marker-specific units. Mitochondrial concentration in the  
 1251 measurement chamber and the tissue of origin are quantified as (1) a quantity for normalization  
 1252 in functional analyses,  $C_{mtE}$ , and (2) a physiological output that is the result of mitochondrial  
 1253 biogenesis and degradation,  $D_{mtE}$ , respectively (**Table 4**). It is recommended, therefore, to  
 1254 distinguish *experimental mitochondrial concentration*,  $C_{mtE} = mtE/V$  and *physiological*  
 1255 *mitochondrial density*,  $D_{mtE} = mtE/m_X$ . Then mitochondrial density is the amount of  
 1256 mitochondrial elementary components per mass of tissue, which is a biological variable (**Figure**  
 1257 **7**). The experimental variable is mitochondrial density multiplied by sample mass concentration  
 1258 in the measuring chamber,  $C_{mtE} = D_{mtE} \cdot C_{mX}$ , or mitochondrial content multiplied by sample  
 1259 number concentration,  $C_{mtE} = mtE_X \cdot C_{NX}$  (**Table 4**).

1260 **mt-Marker-specific flux,  $J_{O_2/mtE}$** : Volume-specific metabolic  $O_2$  flux depends on: (1) the  
 1261 sample concentration in the volume of the instrument chamber,  $C_{mX}$ , or  $C_{NX}$ ; (2) the  
 1262 mitochondrial density in the sample,  $D_{mtE} = mtE/m_X$  or  $mtE_X = mtE/N_X$ ; and (3) the specific  
 1263 mitochondrial activity or performance per elementary mitochondrial unit,  $J_{O_2/mtE} = J_{V,O_2}/C_{mtE}$   
 1264 [ $\text{mol}\cdot\text{s}^{-1}\cdot\text{mtEU}^{-1}$ ] (**Table 4**). Obviously, the numerical results for  $J_{O_2/mtE}$  vary with the type of  
 1265 mitochondrial marker chosen for measurement of *mtE* and  $C_{mtE} = mtE/V$  [ $\text{mtEU}\cdot\text{m}^{-3}$ ].

1266 Different methods are implicated in the quantification of mitochondrial markers and have  
 1267 different strengths. Some problems are common for all mitochondrial markers, *mtE*: (1)  
 1268 Accuracy of measurement is crucial, since even a highly accurate and reproducible  
 1269 measurement of  $O_2$  flux results in an inaccurate and noisy expression if normalized by a biased  
 1270 and noisy measurement of a mitochondrial marker. This problem is acute in mitochondrial  
 1271 respiration because the denominators used (the mitochondrial markers) are often small moieties  
 1272 of which accurate and precise determination is difficult. This problem can be avoided when  $O_2$   
 1273 fluxes measured in substrate-uncoupler-inhibitor titration protocols are normalized for flux in  
 1274 a defined respiratory reference state, which is used as an *internal* marker and yields flux control  
 1275 ratios, *FCRs*. *FCRs* are independent of *externally* measured markers and, therefore, are  
 1276 statistically robust, considering the limitations of ratios in general (Jasienski and Bazzaz 1999).  
 1277 *FCRs* indicate qualitative changes of mitochondrial respiratory control, with highest  
 1278 quantitative resolution, separating the effect of mitochondrial density or concentration on  $J_{O_2/mX}$   
 1279 and  $I_{O_2/NX}$  from that of function per elementary mitochondrial marker,  $J_{O_2/mtE}$  (Pesta *et al.* 2011;  
 1280 Gnaiger 2014). (2) If mitochondrial quality does not change and only the amount of  
 1281 mitochondria varies as a determinant of mass-specific flux, any marker is equally qualified in  
 1282 principle; then in practice selection of the optimum marker depends only on the accuracy and  
 1283 precision of measurement of the mitochondrial marker. (3) If mitochondrial flux control ratios  
 1284 change, then there may not be any best mitochondrial marker. In general, measurement of  
 1285 multiple mitochondrial markers enables a comparison and evaluation of normalization for a  
 1286 variety of mitochondrial markers. Particularly during postnatal development, the activity of  
 1287 marker enzymes—such as cytochrome *c* oxidase and citrate synthase—follows different time

1288 courses (Drahota *et al.* 2004). Evaluation of mitochondrial markers in healthy controls is  
1289 insufficient for providing guidelines for application in the diagnosis of pathological states and  
1290 specific treatments.

1291 In line with the concept of the respiratory control ratio (Chance and Williams 1955a), the  
1292 most readily used normalization is that of flux control ratios and flux control factors (Gnaiger  
1293 2014). Selection of the state of maximum flux in a protocol as the reference state has the  
1294 advantages of: (1) internal normalization; (2) statistically validated linearization of the response  
1295 in the range of 0 to 1; and (3) consideration of maximum flux for integrating a large number of  
1296 elementary steps in the OXPHOS- or ET-pathways. This reduces the risk of selecting a  
1297 functional marker that is specifically altered by the treatment or pathology, yet increases the  
1298 chance that the highly integrative pathway is disproportionately affected, *e.g.*, the OXPHOS-  
1299 rather than ET-pathway in case of an enzymatic defect in the phosphorylation-pathway. In this  
1300 case, additional information can be obtained by reporting flux control ratios based on a  
1301 reference state which indicates stable tissue-mass specific flux.

1302 Stereological determination of mitochondrial content via two-dimensional transmission  
1303 electron microscopy can have limitations due to the dynamics of mitochondrial size (Meinild  
1304 Lundby *et al.* 2017). Accurate determination of three-dimensional volume by two-dimensional  
1305 microscopy can be both time consuming and statistically challenging (Larsen *et al.* 2012).

1306 The validity of using mitochondrial marker enzymes (citrate synthase activity, CI to CIV  
1307 amount or activity) for normalization of flux is limited in part by the same factors that apply to  
1308 flux control ratios. Strong correlations between various mitochondrial markers and citrate  
1309 synthase activity (Reichmann *et al.* 1985; Boushel *et al.* 2007; Mogensen *et al.* 2007) are  
1310 expected in a specific tissue of healthy persons and in disease states not specifically targeting  
1311 citrate synthase. Citrate synthase activity is acutely modifiable by exercise (Tonkonogi *et al.*  
1312 1997; Leek *et al.* 2001). Evaluation of mitochondrial markers related to a selected age and sex  
1313 cohort cannot be extrapolated to provide recommendations for normalization in respirometric  
1314 diagnosis of disease, in different states of development and ageing, different cell types, tissues,  
1315 and species. mtDNA normalized to nDNA via qPCR is correlated to functional mitochondrial  
1316 markers including OXPHOS- and ET-capacity in some cases (Puntschart *et al.* 1995; Wang *et al.*  
1317 1999; Menshikova *et al.* 2006; Boushel *et al.* 2007; Ehinger *et al.* 2015), but lack of such  
1318 correlations have been reported (Menshikova *et al.* 2005; Schultz and Wiesner 2000; Pesta *et al.*  
1319 2011). Several studies indicate a strong correlation between cardiolipin content and increase  
1320 in mitochondrial function with exercise (Menshikova *et al.* 2005; Menshikova *et al.* 2007;  
1321 Larsen *et al.* 2012; Faber *et al.* 2014), but it has not been evaluated as a general mitochondrial  
1322 biomarker in disease. With no single best mitochondrial marker, a good strategy is to quantify  
1323 several different biomarkers to minimize the decorrelating effects caused by diseases,  
1324 treatments, or other factors. Determination of multiple markers, particularly a matrix marker  
1325 and a marker from the mtIM, allows tracking changes in mitochondrial quality defined by their  
1326 ratio.

1327

1328

## 1329 **5. Normalization of rate per system**

1330

### 1331 *5.1. Flow: per chamber*

1332

1333 The experimental system (experimental chamber) is part of the measurement instrument,  
1334 separated from the environment as an isolated, closed, open, isothermal or non-isothermal  
1335 system (**Table 4**). Reporting O<sub>2</sub> flows per respiratory chamber,  $I_{O_2}$  [nmol·s<sup>-1</sup>], restricts the  
1336 analysis to intra-experimental comparison of relative differences.

1337

1338

## 1339 5.2. Flux: per chamber volume

1340  
 1341 **System-specific flux,  $J_{V,O_2}$ :** We distinguish between (1) the *system* with volume  $V$  and  
 1342 mass  $m$  defined by the system boundaries, and (2) the *sample* or *objects* with volume  $V_X$  and  
 1343 mass  $m_X$  that are enclosed in the experimental chamber (Figure 7). Metabolic  $O_2$  flow per  
 1344 object,  $I_{O_2/N_X}$ , is the total  $O_2$  flow in the system divided by the number of objects,  $N_X$ , in the  
 1345 system.  $I_{O_2/N_X}$  increases as the mass of the object is increased. Sample mass-specific  $O_2$  flux,  
 1346  $J_{O_2/m_X}$  should be independent of the mass of the sample studied in the instrument chamber, but  
 1347 system volume-specific  $O_2$  flux,  $J_{V,O_2}$  (per volume of the instrument chamber), increases in  
 1348 proportion to the mass of the sample in the chamber. Whereas  $J_{V,O_2}$  depends on mass-  
 1349 concentration of the sample in the chamber, it should be independent of the chamber (system)  
 1350 volume at constant sample mass. There are practical limitations to increase the mass-  
 1351 concentration of the sample in the chamber, when one is concerned about crowding effects and  
 1352 instrumental time resolution.

1353 **Advancement per volume:** When the reactor volume does not change during the  
 1354 reaction, which is typical for liquid phase reactions, the volume-specific flux of a chemical  
 1355 reaction  $r$  is the time derivative of the advancement of the reaction per unit volume,  $J_{V,r} =$   
 1356  $d\xi_B/dt \cdot V^{-1}$  [(mol·s<sup>-1</sup>)·L<sup>-1</sup>]. The rate of concentration change is  $dc_B/dt$  [(mol·L<sup>-1</sup>)·s<sup>-1</sup>], where  
 1357 concentration is  $c_B = n_B/V$ . There is a difference between (1)  $J_{V,r,O_2}$  [mol·s<sup>-1</sup>·L<sup>-1</sup>] and (2) rate of  
 1358 concentration change [mol·L<sup>-1</sup>·s<sup>-1</sup>]. These merge to a single expression only in closed systems.  
 1359 In open systems, external fluxes (such as  $O_2$  supply) are distinguished from internal  
 1360 transformations (catabolic flux,  $O_2$  consumption). In a closed system, external flows of all  
 1361 substances are zero and  $O_2$  consumption (internal flow of catabolic reactions  $k$ ),  $I_{k,O_2}$  [pmol·s<sup>-1</sup>],  
 1362 causes a decline of the amount of  $O_2$  in the system,  $n_{O_2}$  [nmol]. Normalization of these quantities  
 1363 for the volume of the system,  $V$  [L  $\equiv$  dm<sup>3</sup>], yields volume-specific  $O_2$  flux,  $J_{V,k,O_2} = I_{k,O_2}/V$   
 1364 [nmol·s<sup>-1</sup>·L<sup>-1</sup>], and  $O_2$  concentration,  $[O_2]$  or  $c_{O_2} = n_{O_2}/V$  [ $\mu$ mol·L<sup>-1</sup> =  $\mu$ M = nmol·mL<sup>-1</sup>].  
 1365 Instrumental background  $O_2$  flux is due to external flux into a non-ideal closed respirometer;  
 1366 then total volume-specific flux has to be corrected for instrumental background  $O_2$  flux— $O_2$   
 1367 diffusion into or out of the instrumental chamber.  $J_{V,k,O_2}$  is relevant mainly for methodological  
 1368 reasons and should be compared with the accuracy of instrumental resolution of background-  
 1369 corrected flux, e.g.,  $\pm 1$  nmol·s<sup>-1</sup>·L<sup>-1</sup> (Gnaiger 2001). ‘Metabolic’ or catabolic indicates  $O_2$  flux,  
 1370  $J_{k,O_2}$ , corrected for: (1) instrumental background  $O_2$  flux; (2) chemical background  $O_2$  flux due  
 1371 to autoxidation of chemical components added to the incubation medium; and (3) *Rox* for  $O_2$ -  
 1372 consuming side reactions unrelated to the catabolic pathway  $k$ .

## 1373 1374 1375 6. Conversion of units

1376  
 1377 Many different units have been used to report the  $O_2$  consumption rate, OCR (Table 6).  
 1378 *SI* base units provide the common reference to introduce the theoretical principles (Figure 7),  
 1379 and are used with appropriately chosen *SI* prefixes to express numerical data in the most  
 1380 practical format, with an effort towards unification within specific areas of application (Table  
 1381 7). Reporting data in *SI* units—including the mole [mol], coulomb [C], joule [J], and second  
 1382 [s]—should be encouraged, particularly by journals which propose the use of *SI* units.

1383 Although volume is expressed as m<sup>3</sup> using the *SI* base unit, the litre [dm<sup>3</sup>] is a  
 1384 conventional unit of volume for concentration and is used for most solution chemical kinetics.  
 1385 If one multiplies  $I_{O_2/N_{ce}}$  by  $C_{N_{ce}}$ , then the result will not only be the amount of  $O_2$  [mol]  
 1386 consumed per time [s<sup>-1</sup>] in one litre [L<sup>-1</sup>], but also the change in  $O_2$  concentration per second  
 1387 (for any volume of an ideally closed system). This is ideal for kinetic modeling as it blends with  
 1388 chemical rate equations where concentrations are typically expressed in mol·L<sup>-1</sup> (Wagner *et al.*  
 1389 2011). In studies of multinuclear cells—such as differentiated skeletal muscle cells—it is easy

1390 to determine the number of nuclei but not the total number of cells. A generalized concept,  
 1391 therefore, is obtained by substituting cells by nuclei as the sample entity. This does not hold,  
 1392 however, for enucleated platelets.

1393  
 1394  
 1395  
 1396  
 1397

**Table 6. Conversion of various formats and units used in respirometry and ergometry.**  $e^-$  is the number of electrons or reducing equivalents.  $z_B$  is the charge number of entity B.

Format	1 Unit		Multiplication factor	SI-unit	Notes
$\underline{n}$	ng.atom O $\cdot$ s $^{-1}$	(2 e $^-$ )	0.5	nmol O $_2$ $\cdot$ s $^{-1}$	
$\underline{n}$	ng.atom O $\cdot$ min $^{-1}$	(2 e $^-$ )	8.33	pmol O $_2$ $\cdot$ s $^{-1}$	
$\underline{n}$	natom O $\cdot$ min $^{-1}$	(2 e $^-$ )	8.33	pmol O $_2$ $\cdot$ s $^{-1}$	
$\underline{n}$	nmol O $_2$ $\cdot$ min $^{-1}$	(4 e $^-$ )	16.67	pmol O $_2$ $\cdot$ s $^{-1}$	
$\underline{n}$	nmol O $_2$ $\cdot$ h $^{-1}$	(4 e $^-$ )	0.2778	pmol O $_2$ $\cdot$ s $^{-1}$	
$\underline{V}$ to $\underline{n}$	mL O $_2$ $\cdot$ min $^{-1}$ at STPD $^a$		0.744	$\mu$ mol O $_2$ $\cdot$ s $^{-1}$	1
$\underline{e}$ to $\underline{n}$	W = J/s at -470 kJ/mol O $_2$		-2.128	$\mu$ mol O $_2$ $\cdot$ s $^{-1}$	
$\underline{e}$ to $\underline{n}$	mA = mC $\cdot$ s $^{-1}$	( $z_{H^+} = 1$ )	10.36	nmol H $^+$ $\cdot$ s $^{-1}$	2
$\underline{e}$ to $\underline{n}$	mA = mC $\cdot$ s $^{-1}$	( $z_{O_2} = 4$ )	2.59	nmol O $_2$ $\cdot$ s $^{-1}$	2
$\underline{n}$ to $\underline{e}$	nmol H $^+$ $\cdot$ s $^{-1}$	( $z_{H^+} = 1$ )	0.09649	mA	3
$\underline{n}$ to $\underline{e}$	nmol O $_2$ $\cdot$ s $^{-1}$	( $z_{O_2} = 4$ )	0.38594	mA	3

- 1398 1 At standard temperature and pressure dry (STPD: 0 °C = 273.15 K and 1 atm = 101.325  
 1399 kPa = 760 mmHg), the molar volume of an ideal gas,  $V_m$ , and  $V_{m,O_2}$  is 22.414 and 22.392  
 1400 L $\cdot$ mol $^{-1}$ , respectively. Rounded to three decimal places, both values yield the conversion  
 1401 factor of 0.744. For comparison at normal temperature and pressure dry (NTPD: 20 °C),  
 1402  $V_{m,O_2}$  is 24.038 L $\cdot$ mol $^{-1}$ . Note that the SI standard pressure is 100 kPa.  
 1403 2 The multiplication factor is  $10^6/(z_B \cdot F)$ .  
 1404 3 The multiplication factor is  $z_B \cdot F/10^6$ .  
 1405

1406 For studies of cells, we recommend that respiration be expressed, as far as possible, as:  
 1407 (1) O $_2$  flux normalized for a mitochondrial marker, for separation of the effects of mitochondrial  
 1408 quality and content on cell respiration (this includes FCRs as a normalization for a functional  
 1409 mitochondrial marker); (2) O $_2$  flux in units of cell volume or mass, for comparison of respiration  
 1410 of cells with different cell size (Renner *et al.* 2003) and with studies on tissue preparations, and  
 1411 (3) O $_2$  flow in units of attomole ( $10^{-18}$  mol) of O $_2$  consumed in a second by each cell  
 1412 [amol $\cdot$ s $^{-1}$  $\cdot$ cell $^{-1}$ ], numerically equivalent to [pmol $\cdot$ s $^{-1}$  $\cdot$ 10 $^{-6}$  cells]. This convention allows  
 1413 information to be easily used when designing experiments in which O $_2$  flow must be considered.  
 1414 For example, to estimate the volume-specific O $_2$  flux in an instrument chamber that would be  
 1415 expected at a particular cell number concentration, one simply needs to multiply the flow per  
 1416 cell by the number of cells per volume of interest. This provides the amount of O $_2$  [mol]  
 1417 consumed per time [s $^{-1}$ ] per unit volume [L $^{-1}$ ]. At an O $_2$  flow of 100 amol $\cdot$ s $^{-1}$  $\cdot$ cell $^{-1}$  and a cell  
 1418 density of 10 $^9$  cells $\cdot$ L $^{-1}$  (10 $^6$  cells $\cdot$ mL $^{-1}$ ), the volume-specific O $_2$  flux is 100 nmol $\cdot$ s $^{-1}$  $\cdot$ L $^{-1}$  (100  
 1419 pmol $\cdot$ s $^{-1}$  $\cdot$ mL $^{-1}$ ).

1420 ET-capacity in human cell types including HEK 293, primary HUVEC and fibroblasts  
 1421 ranges from 50 to 180 amol $\cdot$ s $^{-1}$  $\cdot$ cell $^{-1}$ , measured in intact cells in the noncoupled state (see  
 1422 Gnaiger 2014). At 100 amol $\cdot$ s $^{-1}$  $\cdot$ cell $^{-1}$  corrected for  $R_{ox}$ , the current across the mt-membranes,  
 1423  $I_{H^+e}$ , approximates 193 pA $\cdot$ cell $^{-1}$  or 0.2 nA per cell. See Rich (2003) for an extension of  
 1424 quantitative bioenergetics from the molecular to the human scale, with a transmembrane proton  
 1425 flux equivalent to 520 A in an adult at a catabolic power of -110 W. Modelling approaches  
 1426 illustrate the link between protonmotive force and currents (Willis *et al.* 2016).

1427 **Table 7. Conversion of units with preservation of numerical values.**

Name	Frequently used unit	Equivalent unit	Notes
volume-specific flux, $J_{V,O_2}$	$\text{pmol}\cdot\text{s}^{-1}\cdot\text{mL}^{-1}$ $\text{mmol}\cdot\text{s}^{-1}\cdot\text{L}^{-1}$	$\text{nmol}\cdot\text{s}^{-1}\cdot\text{L}^{-1}$ $\text{mol}\cdot\text{s}^{-1}\cdot\text{m}^{-3}$	1
cell-specific flow, $I_{O_2/\text{cell}}$	$\text{pmol}\cdot\text{s}^{-1}\cdot 10^{-6}$ cells	$\text{amol}\cdot\text{s}^{-1}\cdot\text{cell}^{-1}$	2
	$\text{pmol}\cdot\text{s}^{-1}\cdot 10^{-9}$ cells	$\text{zmol}\cdot\text{s}^{-1}\cdot\text{cell}^{-1}$	3
cell number concentration, $C_{N_{\text{ce}}}$	$10^6$ cells $\cdot\text{mL}^{-1}$	$10^9$ cells $\cdot\text{L}^{-1}$	
mitochondrial protein concentration, $C_{mtE}$	$0.1$ mg $\cdot\text{mL}^{-1}$	$0.1$ g $\cdot\text{L}^{-1}$	
mass-specific flux, $J_{O_2/m}$	$\text{pmol}\cdot\text{s}^{-1}\cdot\text{mg}^{-1}$	$\text{nmol}\cdot\text{s}^{-1}\cdot\text{g}^{-1}$	4
catabolic power, $P_k$	$\mu\text{W}\cdot 10^{-6}$ cells	$\text{pW}\cdot\text{cell}^{-1}$	1
Volume	1,000 L	$\text{m}^3$ (1,000 kg)	
	L	$\text{dm}^3$ (kg)	
	mL	$\text{cm}^3$ (g)	
	$\mu\text{L}$	$\text{mm}^3$ (mg)	
	fL	$\mu\text{m}^3$ (pg)	5
amount of substance concentration	$\text{M} = \text{mol}\cdot\text{L}^{-1}$	$\text{mol}\cdot\text{dm}^{-3}$	

1428

1429 1 pmol: picomole =  $10^{-12}$  mol1430 2 amol: attomole =  $10^{-18}$  mol1431 3 zmol: zeptomole =  $10^{-21}$  mol

1432

1433 We consider isolated mitochondria as powerhouses and proton pumps as molecular  
 1434 machines to relate experimental results to energy metabolism of the intact cell. The cellular  
 1435  $P_{\gg}/O_2$  based on oxidation of glycogen is increased by the glycolytic (fermentative) substrate-  
 1436 level phosphorylation of 3  $P_{\gg}/\text{Glyc}$  or 0.5 mol  $P_{\gg}$  for each mol  $O_2$  consumed in the complete  
 1437 oxidation of a mol glycosyl unit (Glyc). Adding 0.5 to the mitochondrial  $P_{\gg}/O_2$  ratio of 5.4  
 1438 yields a bioenergetic cell physiological  $P_{\gg}/O_2$  ratio close to 6. Two NADH equivalents are  
 1439 formed during glycolysis and transported from the cytosol into the mitochondrial matrix, either  
 1440 by the malate-aspartate shuttle or by the glycerophosphate shuttle (**Figure 2A**) resulting in  
 1441 different theoretical yields of ATP generated by mitochondria, the energetic cost of which  
 1442 potentially must be taken into account. Considering also substrate-level phosphorylation in the  
 1443 TCA cycle, this high  $P_{\gg}/O_2$  ratio not only reflects proton translocation and OXPHOS studied  
 1444 in isolation, but integrates mitochondrial physiology with energy transformation in the living  
 1445 cell (Gnaiger 1993a).

1446

1447

1448 **7. Conclusions**

1449

1450 Catabolic cell respiration is the process of exergonic and exothermic energy  
 1451 transformation in which scalar redox reactions are coupled to vectorial ion translocation across  
 1452 a semipermeable membrane, which separates the small volume of a bacterial cell or  
 1453 mitochondrion from the larger volume of its surroundings. The electrochemical exergy can be  
 1454 partially conserved in the phosphorylation of ADP to ATP or in ion pumping, or dissipated in  
 1455 an electrochemical short-circuit. Respiration is thus clearly distinguished from fermentation as  
 1456 the counterpart of cellular core energy metabolism. An  $O_2$  flux balance scheme illustrates the  
 1457 relationships and general definitions (**Figures 1 and 2**).

1458 Experimentally, respiration is separated in mitochondrial preparations from the  
 1459 interactions with the fermentative pathways of the intact cell. OXPHOS analysis (**Figure 3**) is  
 1460 based on the study of mitochondrial preparations complementary to bioenergetic investigations



1461 of intact cells and organisms—from model organisms to the human species including healthy  
 1462 and diseased persons (patients). Different mechanisms of respiratory uncoupling have to be  
 1463 distinguished (**Figure 4**). Metabolic fluxes measured in defined coupling and pathway control  
 1464 states (**Figures 5 and 6**) provide insights into the meaning of cellular and organismic  
 1465 respiration.

1466 The optimal choice for expressing mitochondrial and cell respiration as O<sub>2</sub> flow per  
 1467 biological sample, and normalization for specific tissue-markers (volume, mass, protein) and  
 1468 mitochondrial markers (volume, protein, content, mtDNA, activity of marker enzymes,  
 1469 respiratory reference state) is guided by the scientific question under study. Interpretation of  
 1470 the data depends critically on appropriate normalization (**Figure 7**).

1471 MitoEAGLE can serve as a gateway to better diagnose mitochondrial respiratory  
 1472 adaptations and defects linked to genetic variation, age-related health risks, sex-specific  
 1473 mitochondrial performance, lifestyle with its effects on degenerative diseases, and thermal and  
 1474 chemical environment. The present recommendations on coupling control states and rates,  
 1475 linked to the concept of the protonmotive force, are focused on studies with mitochondrial  
 1476 preparations (**Box 3**). These will be extended in a series of reports on pathway control of  
 1477 mitochondrial respiration, respiratory states in intact cells, and harmonization of experimental  
 1478 procedures.

1479

---

### 1480 **Box 3: Recommendations for studies with mitochondrial preparations**

1481

- 1482 ● Normalization of respiratory rates should be provided as far as possible:
  - 1483 1. *Biophysical normalization*: on a per cell basis as O<sub>2</sub> flow; this may not be possible  
 1484 when dealing with coenocytic organisms or tissues without cross-walls  
 1485 separating individual cells (*e.g.*, filamentous fungi, muscle fibers)
  - 1486 2. *Cellular normalization*: per g protein; per cell- or tissue-mass as mass-specific  
 1487 O<sub>2</sub> flux; per cell volume as cell volume-specific flux
  - 1488 3. *Mitochondrial normalization*: per mitochondrial marker as mt-specific flux.

1489 With information on cell size and the use of multiple normalizations, maximum potential  
 1490 information is available (Renner *et al.* 2003; Wagner *et al.* 2011; Gnaiger 2014). Reporting  
 1491 flow in a respiratory chamber [nmol·s<sup>-1</sup>] is discouraged, since it restricts the analysis to intra-  
 1492 experimental comparison of relative (qualitative) differences.

- 1493 ● Catabolic mitochondrial respiration is distinguished from residual O<sub>2</sub> consumption. Fluxes  
 1494 in mitochondrial coupling states should be, as far as possible, corrected for residual O<sub>2</sub>  
 1495 consumption.

- 1496 ● Different mechanisms of uncoupling should be distinguished by defined terms. The tightness  
 1497 of coupling relates to these uncoupling mechanisms, whereas the coupling stoichiometry  
 1498 varies as a function the substrate type involved in ET-pathways with either three or two  
 1499 redox proton pumps operating in series. Separation of tightness of coupling from the  
 1500 pathway-dependent coupling stoichiometry is possible only when the substrate type  
 1501 undergoing oxidation remains the same for respiration in LEAK-, OXPHOS-, and ET-states.  
 1502 In studies of the tightness of coupling, therefore, simple substrate-inhibitor combinations  
 1503 should be applied to exclude a shift in substrate competition which may occur when  
 1504 providing physiological substrate cocktails.

- 1505 ● In studies of isolated mitochondria, the mitochondrial recovery and yield should be reported.  
 1506 Experimental criteria for evaluation of purity versus integrity should be considered.  
 1507 Mitochondrial markers—such as citrate synthase activity as an enzymatic matrix marker—  
 1508 provide a link to the tissue of origin on the basis of calculating the mitochondrial recovery,  
 1509 *i.e.*, the fraction of mitochondrial marker obtained from a unit mass of tissue. Total  
 1510 mitochondrial protein is frequently applied as a mitochondrial marker, which is restricted to  
 1511 isolated mitochondria.

- 1512 • In studies of permeabilized cells, the viability of the cell culture or cell suspension of origin  
 1513 should be reported. Normalization should be evaluated for total cell count or viable cell  
 1514 count.
- 1515 • Terms and symbols are summarized in **Table 8**. Their use will facilitate transdisciplinary  
 1516 communication and support further developments towards a consistent theory of  
 1517 bioenergetics and mitochondrial physiology. Technical terms related to and defined with  
 1518 normal words can be used as index terms in databases, support the creation of ontologies  
 1519 towards semantic information processing (MitoPedia), and help in communicating analytical  
 1520 findings as impactful data-driven stories. ‘*Making data available without making it*  
 1521 *understandable may be worse than not making it available at all*’ (National Academies of  
 1522 Sciences, Engineering, and Medicine 2018). Success will depend on taking next steps: (1)  
 1523 exhaustive text-mining considering Omics data and functional data; (2) network analysis of  
 1524 Omics data with bioinformatics tools; (3) cross-validation with distinct bioinformatics  
 1525 approaches; (4) correlation with functional data; (5) guidelines for biological validation of  
 1526 network data. This is a call to carefully contribute to FAIR principles (Findable, Accessible,  
 1527 Interoperable, Reusable) for the sharing of scientific data.

1529  
 1530  
 1531 **Table 8. Terms, symbols, and units.**

1532 Term	1533 Symbol	1534 Unit	1535 Links and comments
1536 alternative quinol oxidase	1537 AOX		1538 Figure 2B
1539 amount of substance B	1540 $n_B$	1541 [mol]	
1542 ATP yield per O <sub>2</sub>	1543 $Y_{P_{\text{ATP}}/O_2}$		1544 P <sub>ATP</sub> /O <sub>2</sub> ratio measured in any respiratory 1545 state
1546 catabolic reaction	1547 k		1548 Figure 1 and 3
1549 catabolic respiration	1550 $J_{kO_2}$	1551 <i>varies</i>	1552 Figure 1 and 3
1553 cell number	1554 $N_{ce}$	1555 [x]	1556 Table 5; $N_{ce} = N_{vce} + N_{dce}$
1557 cell respiration	1558 $J_{rO_2}$	1559 <i>varies</i>	1560 Figure 1
1561 cell viability index	1562 VI		1563 $VI = N_{vce}/N_{ce} = 1 - N_{dce}/N_{ce}$
1564 Complexes I to IV	1565 CI to CIV		1566 respiratory ET Complexes; Figure 2B
1567 concentration of substance B	1568 $c_B = n_B \cdot V^{-1}$ ; [B]	1569 [mol·m <sup>-3</sup> ]	1570 Box 2
1571 dead cell number	1572 $N_{dce}$	1573 [x]	1574 Table 5; non-viable cells, loss of plasma 1575 membrane barrier function
1576 electric format	1577 $e$	1578 [C]	1579 Table 6
1580 electron transfer system	1581 ETS		1582 Figure 2B, Figure 5; state
1583 flow, for substance B	1584 $I_B$	1585 [mol·s <sup>-1</sup> ]	1586 system-related extensive quantity; 1587 Figure 7
1588 flux, for substance B	1589 $J_B$	1590 <i>varies</i>	1591 size-specific quantity; Figure 7
1592 inorganic phosphate	1593 P <sub>i</sub>		1594 Figure 3
1595 intact cell number, viable cell number	1596 $N_{vce}$	1597 [x]	1598 Table 5; viable cells, intact of plasma 1599 membrane barrier function
1600 LEAK	1601 LEAK		1602 Table 1, Figure 5; state
1603 mass format	1604 $m$	1605 [kg]	1606 Table 4, Figure 7
1607 mass of sample X	1608 $m_X$	1609 [kg]	1610 Table 4
1611 mass of entity X	1612 $M_X$	1613 [kg]	1614 mass of object X; Table 4
1615 MITOCARTA			1616 <a href="https://www.broadinstitute.org/scientific-community/science/programs/metabolic-disease-program/publications/mitocarta/mitocarta-in-0">https://www.broadinstitute.org/scientific-community/science/programs/metabolic-disease-program/publications/mitocarta/mitocarta-in-0</a>
1617 MitoPedia			1618 <a href="http://www.bioblast.at/index.php/MitoPedia">http://www.bioblast.at/index.php/MitoPedia</a>
1619 mitochondria or mitochondrial	1620 mt		1621 Box 1
1622 mitochondrial DNA	1623 mtDNA		1624 Box 1
1625 mitochondrial concentration	1626 $C_{mtE} = mtE \cdot V^{-1}$	1627 [mtEU·m <sup>-3</sup> ]	1628 Table 4

1571	mitochondrial content	$mtE_X = mtE \cdot N_X^{-1}$	[mtEU·x <sup>-1</sup> ]	Table 4
1572	mitochondrial elementary component	$mtE$	[mtEU]	Table 4, quantity of mt-marker
1573	mitochondrial elementary unit	mtEU	<i>varies</i>	Table 4, specific units for mt-marker
1574	mitochondrial inner membrane	mtIM		Figure 2; MIM is widely used; the first M is replaced by mt; Box 1
1575				
1576	mitochondrial outer membrane	mtOM		Figure 2; MOM is widely used; the first M is replaced by mt; Box 1
1577				
1578	mitochondrial recovery	$Y_{mtE}$		fraction of $mtE$ recovered in sample from the tissue of origin
1579				
1580	mitochondrial yield	$Y_{mtE/\underline{m}}$		mt-yield per tissues mass; $Y_{mtE/\underline{m}} = Y_{mtE} \cdot D_{mtE}$
1581				
1582	molar format	$\underline{n}$	[mol]	Table 6
1583	negative	neg		Figure 3
1584	number concentration of $X$	$C_{NX}$	[x·m <sup>-3</sup> ]	Table 4
1585	number format	$\underline{N}$	[x]	Table 4, Figure 7
1586	number of entities $X$	$N_X$	[x]	Table 4, Figure 7
1587	number of entity B	$N_B$	[x]	Table 4
1588	oxidative phosphorylation	OXPPOS		Table 1, Figure 5; state
1589	oxygen concentration	$c_{O_2} = n_{O_2} \cdot V^{-1}$ ; [O <sub>2</sub> ]	[mol·m <sup>-3</sup> ]	Section 3.2
1590	oxygen flux, in reaction r	$J_{rO_2}$	<i>varies</i>	Figure 1
1591	permeabilized cell number	$N_{pce}$	[x]	Table 5; experimental permeabilization of plasma membrane; $N_{pce} = N_{ce}$
1592				
1593	phosphorylation of ADP to ATP	P»		Section 2.2
1594	positive	pos		Figure 3
1595	proton in the negative compartment	H <sup>+</sup> <sub>neg</sub>		Figure 3
1596	proton in the positive compartment	H <sup>+</sup> <sub>pos</sub>		Figure 3
1597	rate of electron transfer in ET state	$E$		ET-capacity; Table 1
1598	rate of LEAK respiration	$L$		Table 1
1599	rate of oxidative phosphorylation	$P$		OXPPOS capacity; Table 1
1600	rate of residual oxygen consumption	$RoX$		Table 1, Figure 1
1601	residual oxygen consumption	ROX		Table 1; state
1602	respiratory supercomplex	SC I <sub>n</sub> III <sub>n</sub> IV <sub>n</sub>		Box 1; supramolecular assemblies composed of variable copy numbers ( $n$ ) of CI, CIII and CIV
1603				
1604				
1605	specific mitochondrial density	$D_{mtE} = mtE \cdot m_X^{-1}$	[mtEU·kg <sup>-1</sup> ]	Table 4
1606	volume	$V$	[m <sup>-3</sup> ]	Table 7
1607	volume format	$\underline{V}$	[m <sup>-3</sup> ]	Table 6
1608	weight, dry weight	$W_d$	[kg]	used as mass of sample $X$ ; Figure 7
1609	weight, wet weight	$W_w$	[kg]	used as mass of sample $X$ ; Figure 7
1610				

1611

## Acknowledgements

1612 We thank M. Beno for management assistance. This publication is based upon work from  
 1613 COST Action CA15203 MitoEAGLE, supported by COST (European Cooperation in Science  
 1614 and Technology), and K-Regio project MitoFit (E.G.).

1615

1616  
 1617 **Competing financial interests:** E.G. is founder and CEO of Oroboros Instruments, Innsbruck,  
 1618 Austria.

1619

## References

1620

1621 Altmann R (1894) Die Elementarorganismen und ihre Beziehungen zu den Zellen. Zweite vermehrte Auflage.  
 1622 Verlag Von Veit & Comp, Leipzig:160 pp.

1623 Baggeto LG, Testa-Perussini R (1990) Role of acetoin on the regulation of intermediate metabolism of Ehrlich  
 1624 ascites tumor mitochondria: its contribution to membrane cholesterol enrichment modifying passive proton  
 1625 permeability. Arch Biochem Biophys 283:341-8.

1626 Beard DA (2005) A biophysical model of the mitochondrial respiratory system and oxidative phosphorylation.  
 1627 PLoS Comput Biol 1(4):e36.

1628 Benda C (1898) Weitere Mitteilungen über die Mitochondria. Verh Dtsch Physiol Ges:376-83.

1629

- 1630 Birkedal R, Laasmaa M, Vendelin M (2014) The location of energetic compartments affects energetic  
1631 communication in cardiomyocytes. *Front Physiol* 5:376.
- 1632 Blier PU, Dufresne F, Burton RS (2001) Natural selection and the evolution of mtDNA-encoded peptides:  
1633 evidence for intergenomic co-adaptation. *Trends Genet* 17:400-6.
- 1634 Blier PU, Guderley HE (1993) Mitochondrial activity in rainbow trout red muscle: the effect of temperature on  
1635 the ADP-dependence of ATP synthesis. *J Exp Biol* 176:145-58.
- 1636 Breton S, Beaupré HD, Stewart DT, Hoeh WR, Blier PU (2007) The unusual system of doubly uniparental  
1637 inheritance of mtDNA: isn't one enough? *Trends Genet* 23:465-74.
- 1638 Brown GC (1992) Control of respiration and ATP synthesis in mammalian mitochondria and cells. *Biochem J*  
1639 284:1-13.
- 1640 Calvo SE, Klauser CR, Mootha VK (2016) MitoCarta2.0: an updated inventory of mammalian mitochondrial  
1641 proteins. *Nucleic Acids Research* 44:D1251-7.
- 1642 Calvo SE, Julien O, Clauser KR, Shen H, Kamer KJ, Wells JA, Mootha VK (2017) Comparative analysis of  
1643 mitochondrial N-termini from mouse, human, and yeast. *Mol Cell Proteomics* 16:512-23.
- 1644 Campos JC, Queliconi BB, Bozi LHM, Bechara LRG, Dourado PMM, Andres AM, Jannig PR, Gomes KMS,  
1645 Zambelli VO, Rocha-Resende C, Guatimosim S, Brum PC, Mochly-Rosen D, Gottlieb RA, Kowaltowski AJ,  
1646 Ferreira JCB (2017) Exercise reestablishes autophagic flux and mitochondrial quality control in heart failure.  
1647 *Autophagy* 13:1304-317.
- 1648 Canton M, Luvisetto S, Schmehl I, Azzone GF (1995) The nature of mitochondrial respiration and  
1649 discrimination between membrane and pump properties. *Biochem J* 310:477-81.
- 1650 Carrico C, Meyer JG, He W, Gibson BW, Verdin E (2018) The mitochondrial acylome emerges: proteomics,  
1651 regulation by Sirtuins, and metabolic and disease implications. *Cell Metab* 27:497-512.
- 1652 Chan DC (2006) Mitochondria: dynamic organelles in disease, aging, and development. *Cell* 125:1241-52.
- 1653 Chance B, Williams GR (1955a) Respiratory enzymes in oxidative phosphorylation. I. Kinetics of oxygen  
1654 utilization. *J Biol Chem* 217:383-93.
- 1655 Chance B, Williams GR (1955b) Respiratory enzymes in oxidative phosphorylation: III. The steady state. *J Biol*  
1656 *Chem* 217:409-27.
- 1657 Chance B, Williams GR (1955c) Respiratory enzymes in oxidative phosphorylation. IV. The respiratory chain. *J*  
1658 *Biol Chem* 217:429-38.
- 1659 Chance B, Williams GR (1956) The respiratory chain and oxidative phosphorylation. *Adv Enzymol Relat Subj*  
1660 *Biochem* 17:65-134.
- 1661 Chowdhury SK, Djordjevic J, Albensi B, Fernyhough P (2015) Simultaneous evaluation of substrate-dependent  
1662 oxygen consumption rates and mitochondrial membrane potential by TMRM and safranin in cortical  
1663 mitochondria. *Biosci Rep* 36:e00286.
- 1664 Cobb LJ, Lee C, Xiao J, Yen K, Wong RG, Nakamura HK, Mehta HH, Gao Q, Ashur C, Huffman DM, Wan J,  
1665 Muzumdar R, Barzilai N, Cohen P (2016) Naturally occurring mitochondrial-derived peptides are age-  
1666 dependent regulators of apoptosis, insulin sensitivity, and inflammatory markers. *Aging (Albany NY)* 8:796-  
1667 809.
- 1668 Cohen ER, Cvitas T, Frey JG, Holmström B, Kuchitsu K, Marquardt R, Mills I, Pavese F, Quack M, Stohner J,  
1669 Strauss HL, Takami M, Thor HL (2008) Quantities, units and symbols in physical chemistry, IUPAC Green  
1670 Book, 3rd Edition, 2nd Printing, IUPAC & RSC Publishing, Cambridge.
- 1671 Cooper H, Hedges LV, Valentine JC, eds (2009) The handbook of research synthesis and meta-analysis. Russell  
1672 Sage Foundation.
- 1673 Coopersmith J (2010) Energy, the subtle concept. The discovery of Feynman's blocks from Leibnitz to Einstein.  
1674 Oxford University Press:400 pp.
- 1675 Cummins J (1998) Mitochondrial DNA in mammalian reproduction. *Rev Reprod* 3:172-82.
- 1676 Dai Q, Shah AA, Garde RV, Yonish BA, Zhang L, Medvitz NA, Miller SE, Hansen EL, Dunn CN, Price TM  
1677 (2013) A truncated progesterone receptor (PR-M) localizes to the mitochondrion and controls cellular  
1678 respiration. *Mol Endocrinol* 27:741-53.
- 1679 Daum B, Walter A, Horst A, Osiewacz HD, Kühlbrandt W (2013) Age-dependent dissociation of ATP synthase  
1680 dimers and loss of inner-membrane cristae in mitochondria. *Proc Natl Acad Sci U S A* 110:15301-6.
- 1681 Divakaruni AS, Brand MD (2011) The regulation and physiology of mitochondrial proton leak. *Physiology*  
1682 (Bethesda) 26:192-205.
- 1683 Doerrier C, Garcia-Souza LF, Krumschnabel G, Wohlfarter Y, Mészáros AT, Gnaiger E (2018) High-Resolution  
1684 Fluorescence Respirometry and OXPHOS protocols for human cells, permeabilized fibres from small biopsies of  
1685 muscle, and isolated mitochondria. *Methods Mol Biol* 1782 (Palmeira CM, Moreno AJ, eds): Mitochondrial  
1686 Bioenergetics, 978-1-4939-7830-4.
- 1687 Doskey CM, van 't Erve TJ, Wagner BA, Buettner GR (2015) Moles of a substance per cell is a highly  
1688 informative dosing metric in cell culture. *PLOS ONE* 10:e0132572.
- 1689 Drahota Z, Milerová M, Stieglarová A, Houstek J, Ostádal B (2004) Developmental changes of cytochrome c  
1690 oxidase and citrate synthase in rat heart homogenate. *Physiol Res* 53:119-22.

- 1691 Duarte FV, Palmeira CM, Rolo AP (2014) The role of microRNAs in mitochondria: small players acting wide.  
1692 *Genes (Basel)* 5:865-86.
- 1693 Ehinger JK, Morota S, Hansson MJ, Paul G, Elmér E (2015) Mitochondrial dysfunction in blood cells from  
1694 amyotrophic lateral sclerosis patients. *J Neurol* 262:1493-503.
- 1695 Ernster L, Schatz G (1981) Mitochondria: a historical review. *J Cell Biol* 91:227s-55s.
- 1696 Estabrook RW (1967) Mitochondrial respiratory control and the polarographic measurement of ADP:O ratios.  
1697 *Methods Enzymol* 10:41-7.
- 1698 Faber C, Zhu ZJ, Castellino S, Wagner DS, Brown RH, Peterson RA, Gates L, Barton J, Bickett M, Hagerty L,  
1699 Kimbrough C, Sola M, Bailey D, Jordan H, Elangbam CS (2014) Cardiolipin profiles as a potential  
1700 biomarker of mitochondrial health in diet-induced obese mice subjected to exercise, diet-restriction and  
1701 ephedrine treatment. *J Appl Toxicol* 34:1122-9.
- 1702 Fell D (1997) Understanding the control of metabolism. Portland Press.
- 1703 Forstner H, Gnaiger E (1983) Calculation of equilibrium oxygen concentration. In: Polarographic Oxygen  
1704 Sensors. Aquatic and Physiological Applications. Gnaiger E, Forstner H (eds), Springer, Berlin, Heidelberg,  
1705 New York:321-33.
- 1706 Garlid KD, Beavis AD, Ratkje SK (1989) On the nature of ion leaks in energy-transducing membranes. *Biochim*  
1707 *Biophys Acta* 976:109-20.
- 1708 Garlid KD, Semrad C, Zinchenko V. Does redox slip contribute significantly to mitochondrial respiration? In:  
1709 Schuster S, Rigoulet M, Ouhabi R, Mazat J-P, eds (1993) Modern trends in biothermokinetics. Plenum Press,  
1710 New York, London:287-93.
- 1711 Gerö D, Szabo C (2016) Glucocorticoids suppress mitochondrial oxidant production via upregulation of  
1712 uncoupling protein 2 in hyperglycemic endothelial cells. *PLoS One* 11:e0154813.
- 1713 Gnaiger E. Efficiency and power strategies under hypoxia. Is low efficiency at high glycolytic ATP production a  
1714 paradox? In: Surviving Hypoxia: Mechanisms of Control and Adaptation. Hochachka PW, Lutz PL, Sick T,  
1715 Rosenthal M, Van den Thillart G, eds (1993a) CRC Press, Boca Raton, Ann Arbor, London, Tokyo:77-109.
- 1716 Gnaiger E (1993b) Nonequilibrium thermodynamics of energy transformations. *Pure Appl Chem* 65:1983-2002.
- 1717 Gnaiger E (2001) Bioenergetics at low oxygen: dependence of respiration and phosphorylation on oxygen and  
1718 adenosine diphosphate supply. *Respir Physiol* 128:277-97.
- 1719 Gnaiger E (2009) Capacity of oxidative phosphorylation in human skeletal muscle. New perspectives of  
1720 mitochondrial physiology. *Int J Biochem Cell Biol* 41:1837-45.
- 1721 Gnaiger E (2014) Mitochondrial pathways and respiratory control. An introduction to OXPHOS analysis. 4th ed.  
1722 *Mitochondr Physiol Network* 19.12. Oroboros MiPNet Publications, Innsbruck:80 pp.
- 1723 Gnaiger E, Méndez G, Hand SC (2000) High phosphorylation efficiency and depression of uncoupled respiration  
1724 in mitochondria under hypoxia. *Proc Natl Acad Sci USA* 97:11080-5.
- 1725 Greggio C, Jha P, Kulkarni SS, Lagarrigue S, Broskey NT, Boutant M, Wang X, Conde Alonso S, Ofori E,  
1726 Auwerx J, Cantó C, Amati F (2017) Enhanced respiratory chain supercomplex formation in response to  
1727 exercise in human skeletal muscle. *Cell Metab* 25:301-11.
- 1728 Hinkle PC (2005) P/O ratios of mitochondrial oxidative phosphorylation. *Biochim Biophys Acta* 1706:1-11.
- 1729 Hofstadter DR (1979) Gödel, Escher, Bach: An eternal golden braid. A metaphorical fugue on minds and  
1730 machines in the spirit of Lewis Carroll. Harvester Press:499 pp.
- 1731 Illaste A, Laasmaa M, Peterson P, Vendelin M (2012) Analysis of molecular movement reveals latticelike  
1732 obstructions to diffusion in heart muscle cells. *Biophys J* 102:739-48.
- 1733 Jasienski M, Bazzaz FA (1999) The fallacy of ratios and the testability of models in biology. *Oikos* 84:321-26.
- 1734 Jepihhina N, Beraud N, Sepp M, Birkedal R, Vendelin M (2011) Permeabilized rat cardiomyocyte response  
1735 demonstrates intracellular origin of diffusion obstacles. *Biophys J* 101:2112-21.
- 1736 Klepinin A, Ounpuu L, Guzun R, Chekulayev V, Timohhina N, Tepp K, Shevchuk I, Schlattner U, Kaambre T  
1737 (2016) Simple oxygraphic analysis for the presence of adenylate kinase 1 and 2 in normal and tumor cells. *J*  
1738 *Bioenerg Biomembr* 48:531-48.
- 1739 Klingenberg M (2017) UCP1 - A sophisticated energy valve. *Biochimie* 134:19-27.
- 1740 Koit A, Shevchuk I, Ounpuu L, Klepinin A, Chekulayev V, Timohhina N, Tepp K, Puurand M, Truu L, Heck K,  
1741 Valvere V, Guzun R, Kaambre T (2017) Mitochondrial respiration in human colorectal and breast cancer  
1742 clinical material is regulated differently. *Oxid Med Cell Longev* 1372640.
- 1743 Komlódi T, Tretter L (2017) Methylene blue stimulates substrate-level phosphorylation catalysed by succinyl-  
1744 CoA ligase in the citric acid cycle. *Neuropharmacology* 123:287-98.
- 1745 Korn E (1969) Cell membranes: structure and synthesis. *Annu Rev Biochem* 38:263-88.
- 1746 Lane N (2005) Power, sex, suicide: mitochondria and the meaning of life. Oxford University Press:354 pp.
- 1747 Larsen S, Nielsen J, Neigaard Nielsen C, Nielsen LB, Wibrand F, Stride N, Schroder HD, Boushel RC, Helge  
1748 JW, Dela F, Hey-Mogensen M (2012) Biomarkers of mitochondrial content in skeletal muscle of healthy  
1749 young human subjects. *J Physiol* 590:3349-60.
- 1750 Lee C, Zeng J, Drew BG, Sallam T, Martin-Montalvo A, Wan J, Kim SJ, Mehta H, Hevener AL, de Cabo R,  
1751 Cohen P (2015) The mitochondrial-derived peptide MOTS-c promotes metabolic homeostasis and reduces  
1752 obesity and insulin resistance. *Cell Metab* 21:443-54.

- 1753 Lee SR, Kim HK, Song IS, Youm J, Dizon LA, Jeong SH, Ko TH, Heo HJ, Ko KS, Rhee BD, Kim N, Han J  
1754 (2013) Glucocorticoids and their receptors: insights into specific roles in mitochondria. *Prog Biophys Mol*  
1755 *Biol* 112:44-54.
- 1756 Leek BT, Mudaliar SR, Henry R, Mathieu-Costello O, Richardson RS (2001) Effect of acute exercise on citrate  
1757 synthase activity in untrained and trained human skeletal muscle. *Am J Physiol Regul Integr Comp Physiol*  
1758 280:R441-7.
- 1759 Lemieux H, Blier PU, Gnaiger E (2017) Remodeling pathway control of mitochondrial respiratory capacity by  
1760 temperature in mouse heart: electron flow through the Q-junction in permeabilized fibers. *Sci Rep* 7:2840.
- 1761 Lenaz G, Tioli G, Falasca AI, Genova ML (2017) Respiratory supercomplexes in mitochondria. In: *Mechanisms*  
1762 *of primary energy transduction in biology*. M Wikstrom (ed) Royal Society of Chemistry Publishing, London,  
1763 UK:296-337.
- 1764 Liu S, Roellig DM, Guo Y, Li N, Frace MA, Tang K, Zhang L, Feng Y, Xiao L (2016) Evolution of mitosome  
1765 metabolism and invasion-related proteins in *Cryptosporidium*. *BMC Genomics* 17:1006.
- 1766 Margulis L (1970) Origin of eukaryotic cells. New Haven: Yale University Press.
- 1767 Meinild Lundby AK, Jacobs RA, Gehrig S, de Leur J, Hauser M, Bonne TC, Flück D, Dandanell S, Kirk N,  
1768 Kaech A, Ziegler U, Larsen S, Lundby C (2018) Exercise training increases skeletal muscle mitochondrial  
1769 volume density by enlargement of existing mitochondria and not de novo biogenesis. *Acta Physiol* 222,  
1770 e12905.
- 1771 Menshikova EV, Ritov VB, Fairfull L, Ferrell RE, Kelley DE, Goodpaster BH (2006) Effects of exercise on  
1772 mitochondrial content and function in aging human skeletal muscle. *J Gerontol A Biol Sci Med Sci* 61:534-  
1773 40.
- 1774 Menshikova EV, Ritov VB, Ferrell RE, Azuma K, Goodpaster BH, Kelley DE (2007) Characteristics of skeletal  
1775 muscle mitochondrial biogenesis induced by moderate-intensity exercise and weight loss in obesity. *J Appl*  
1776 *Physiol* (1985) 103:21-7.
- 1777 Menshikova EV, Ritov VB, Toledo FG, Ferrell RE, Goodpaster BH, Kelley DE (2005) Effects of weight loss  
1778 and physical activity on skeletal muscle mitochondrial function in obesity. *Am J Physiol Endocrinol Metab*  
1779 288:E818-25.
- 1780 Miller GA (1991) The science of words. Scientific American Library New York:276 pp.
- 1781 Mitchell P (1961) Coupling of phosphorylation to electron and hydrogen transfer by a chemi-osmotic type of  
1782 mechanism. *Nature* 191:144-8.
- 1783 Mitchell P (2011) Chemiosmotic coupling in oxidative and photosynthetic phosphorylation. *Biochim Biophys*  
1784 *Acta Bioenergetics* 1807:1507-38.
- 1785 Mogensen M, Sahlin K, Fernström M, Glintborg D, Vind BF, Beck-Nielsen H, Højlund K (2007) Mitochondrial  
1786 respiration is decreased in skeletal muscle of patients with type 2 diabetes. *Diabetes* 56:1592-9.
- 1787 Mohr PJ, Phillips WD (2015) Dimensionless units in the SI. *Metrologia* 52:40-7.
- 1788 Moreno M, Giacco A, Di Munno C, Goglia F (2017) Direct and rapid effects of 3,5-diiodo-L-thyronine (T2).  
1789 *Mol Cell Endocrinol* 7207:30092-8.
- 1790 Morrow RM, Picard M, Derbeneva O, Leipzig J, McManus MJ, Gouspillou G, Barbat-Artigas S, Dos Santos C,  
1791 Hepple RT, Murdock DG, Wallace DC (2017) Mitochondrial energy deficiency leads to hyperproliferation of  
1792 skeletal muscle mitochondria and enhanced insulin sensitivity. *Proc Natl Acad Sci U S A* 114:2705-10.
- 1793 Murley A, Nunnari J (2016) The emerging network of mitochondria-organelle contacts. *Mol Cell* 61:648-53.
- 1794 National Academies of Sciences, Engineering, and Medicine (2018) International coordination for science data  
1795 infrastructure: Proceedings of a workshop—in brief. Washington, DC: The National Academies Press. doi:  
1796 <https://doi.org/10.17226/25015>.
- 1797 Palmfeldt J, Bross P (2017) Proteomics of human mitochondria. *Mitochondrion* 33:2-14.
- 1798 Paradies G, Paradies V, De Benedictis V, Ruggiero FM, Petrosillo G (2014) Functional role of cardiolipin in  
1799 mitochondrial bioenergetics. *Biochim Biophys Acta* 1837:408-17.
- 1800 Pesta D, Gnaiger E (2012) High-Resolution Respirometry. OXPHOS protocols for human cells and  
1801 permeabilized fibres from small biopsies of human muscle. *Methods Mol Biol* 810:25-58.
- 1802 Pesta D, Hoppel F, Macek C, Messner H, Faulhaber M, Kobel C, Parson W, Burtcher M, Schocke M, Gnaiger  
1803 E (2011) Similar qualitative and quantitative changes of mitochondrial respiration following strength and  
1804 endurance training in normoxia and hypoxia in sedentary humans. *Am J Physiol Regul Integr Comp Physiol*  
1805 301:R1078-87.
- 1806 Price TM, Dai Q (2015) The role of a mitochondrial progesterone receptor (PR-M) in progesterone action.  
1807 *Semin Reprod Med* 33:185-94.
- 1808 Puchowicz MA, Varnes ME, Cohen BH, Friedman NR, Kerr DS, Hoppel CL (2004) Oxidative phosphorylation  
1809 analysis: assessing the integrated functional activity of human skeletal muscle mitochondria – case studies.  
1810 *Mitochondrion* 4:377-85. Puntschart A, Claassen H, Jostarndt K, Hoppeler H, Billeter R (1995) mRNAs of  
1811 enzymes involved in energy metabolism and mtDNA are increased in endurance-trained athletes. *Am J*  
1812 *Physiol* 269:C619-25.
- 1813 Quiros PM, Mottis A, Auwerx J (2016) Mitonuclear communication in homeostasis and stress. *Nat Rev Mol*  
1814 *Cell Biol* 17:213-26.

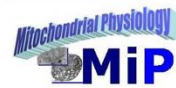
- 1815 Rackham O, Mercer TR, Filipovska A (2012) The human mitochondrial transcriptome and the RNA-binding  
 1816 proteins that regulate its expression. *WIREs RNA* 3:675–95.
- 1817 Reichmann H, Hoppeler H, Mathieu-Costello O, von Bergen F, Pette D (1985) Biochemical and ultrastructural  
 1818 changes of skeletal muscle mitochondria after chronic electrical stimulation in rabbits. *Pflugers Arch* 404:1-  
 1819 9.
- 1820 Renner K, Amberger A, Konwalinka G, Gnaiger E (2003) Changes of mitochondrial respiration, mitochondrial  
 1821 content and cell size after induction of apoptosis in leukemia cells. *Biochim Biophys Acta* 1642:115-23.
- 1822 Rice DW, Alverson AJ, Richardson AO, Young GJ, Sanchez-Puerta MV, Munzinger J, Barry K, Boore JL,  
 1823 Zhang Y, dePamphilis CW, Knox EB, Palmer JD (2016) Horizontal transfer of entire genomes via  
 1824 mitochondrial fusion in the angiosperm *Amborella*. *Science* 342:1468-73.
- 1825 Rich P (2003) Chemiosmotic coupling: The cost of living. *Nature* 421:583.
- 1826 Rich PR (2013) Chemiosmotic theory. *Encyclopedia Biol Chem* 1:467-72.
- 1827 Rostovtseva TK, Sheldon KL, Hassanzadeh E, Monge C, Saks V, Bezrukov SM, Sackett DL (2008) Tubulin  
 1828 binding blocks mitochondrial voltage-dependent anion channel and regulates respiration. *Proc Natl Acad Sci*  
 1829 *USA* 105:18746-51.
- 1830 Rustin P, Parfait B, Chretien D, Bourgeron T, Djouadi F, Bastin J, Rötig A, Munnich A (1996) Fluxes of  
 1831 nicotinamide adenine dinucleotides through mitochondrial membranes in human cultured cells. *J Biol Chem*  
 1832 271:14785-90.
- 1833 Saks VA, Veksler VI, Kuznetsov AV, Kay L, Sikk P, Tiivel T, Tranqui L, Olivares J, Winkler K, Wiedemann F,  
 1834 Kunz WS (1998) Permeabilised cell and skinned fiber techniques in studies of mitochondrial function in  
 1835 vivo. *Mol Cell Biochem* 184:81-100.
- 1836 Salabei JK, Gibb AA, Hill BG (2014) Comprehensive measurement of respiratory activity in permeabilized cells  
 1837 using extracellular flux analysis. *Nat Protoc* 9:421-38.
- 1838 Sazanov LA (2015) A giant molecular proton pump: structure and mechanism of respiratory complex I. *Nat Rev*  
 1839 *Mol Cell Biol* 16:375-88.
- 1840 Schneider TD (2006) Claude Shannon: biologist. The founder of information theory used biology to formulate  
 1841 the channel capacity. *IEEE Eng Med Biol Mag* 25:30-3.
- 1842 Schönfeld P, Dymkowska D, Wojtczak L (2009) Acyl-CoA-induced generation of reactive oxygen species in  
 1843 mitochondrial preparations is due to the presence of peroxisomes. *Free Radic Biol Med* 47:503-9.
- 1844 Schultz J, Wiesner RJ (2000) Proliferation of mitochondria in chronically stimulated rabbit skeletal muscle--  
 1845 transcription of mitochondrial genes and copy number of mitochondrial DNA. *J Bioenerg Biomembr* 32:627-  
 1846 34.
- 1847 Speijer D (2016) Being right on Q: shaping eukaryotic evolution. *Biochem J* 473:4103-27.
- 1848 Sugiura A, Mattie S, Prudent J, McBride HM (2017) Newly born peroxisomes are a hybrid of mitochondrial and  
 1849 ER-derived pre-peroxisomes. *Nature* 542:251-4.
- 1850 Simson P, Jepihhina N, Laasmaa M, Peterson P, Birkedal R, Vendelin M (2016) Restricted ADP movement in  
 1851 cardiomyocytes: Cytosolic diffusion obstacles are complemented with a small number of open mitochondrial  
 1852 voltage-dependent anion channels. *J Mol Cell Cardiol* 97:197-203.
- 1853 Stucki JW, Ineichen EA (1974) Energy dissipation by calcium recycling and the efficiency of calcium transport  
 1854 in rat-liver mitochondria. *Eur J Biochem* 48:365-75.
- 1855 Tonkonogi M, Harris B, Sahlin K (1997) Increased activity of citrate synthase in human skeletal muscle after a  
 1856 single bout of prolonged exercise. *Acta Physiol Scand* 161:435-6.
- 1857 Torralba D, Baixauli F, Sánchez-Madrid F (2016) Mitochondria know no boundaries: mechanisms and functions  
 1858 of intercellular mitochondrial transfer. *Front Cell Dev Biol* 4:107. eCollection 2016.
- 1859 Vamecq J, Schepers L, Parmentier G, Mannaerts GP (1987) Inhibition of peroxisomal fatty acyl-CoA oxidase by  
 1860 antimycin A. *Biochem J* 248:603-7.
- 1861 Waczulikova I, Habodaszova D, Cagalinec M, Ferko M, Ulicna O, Mateasik A, Sikurova L, Ziegelhöffer A  
 1862 (2007) Mitochondrial membrane fluidity, potential, and calcium transients in the myocardium from acute  
 1863 diabetic rats. *Can J Physiol Pharmacol* 85:372-81.
- 1864 Wagner BA, Venkataraman S, Buettner GR (2011) The rate of oxygen utilization by cells. *Free Radic Biol Med*  
 1865 51:700-712.
- 1866 Wang H, Hiatt WR, Barstow TJ, Brass EP (1999) Relationships between muscle mitochondrial DNA content,  
 1867 mitochondrial enzyme activity and oxidative capacity in man: alterations with disease. *Eur J Appl Physiol*  
 1868 *Occup Physiol* 80:22-7.
- 1869 Watt IN, Montgomery MG, Runswick MJ, Leslie AG, Walker JE (2010) Bioenergetic cost of making an  
 1870 adenosine triphosphate molecule in animal mitochondria. *Proc Natl Acad Sci U S A* 107:16823-7.
- 1871 Weibel ER, Hoppeler H (2005) Exercise-induced maximal metabolic rate scales with muscle aerobic capacity. *J*  
 1872 *Exp Biol* 208:1635–44.
- 1873 White DJ, Wolff JN, Pierson M, Gemmell NJ (2008) Revealing the hidden complexities of mtDNA inheritance.  
 1874 *Mol Ecol* 17:4925–42.
- 1875 Wikström M, Hummer G (2012) Stoichiometry of proton translocation by respiratory complex I and its  
 1876 mechanistic implications. *Proc Natl Acad Sci U S A* 109:4431-6.

1877 Williams EG, Wu Y, Jha P, Dubuis S, Blattmann P, Argmann CA, Houten SM, Amariuta T, Wolski W,  
 1878 Zamboni N, Aebersold R, Auwerx J (2016) Systems proteomics of liver mitochondria function. Science 352  
 1879 (6291):aad0189  
 1880 Willis WT, Jackman MR, Messer JI, Kuzmiak-Glancy S, Glancy B (2016) A simple hydraulic analog model of  
 1881 oxidative phosphorylation. Med Sci Sports Exerc 48:990-1000.  
 1882



# Mitochondrial respiratory states and rates:

## Building blocks of mitochondrial physiology



Part 1 - [www.mitoeagle.org/index.php/MitoEAGLE\\_preprint\\_2018-02-08](http://www.mitoeagle.org/index.php/MitoEAGLE_preprint_2018-02-08)

Gnaiger E<sup>1,2</sup>, corresponding author  
 355 co-authors, MitoEAGLE Working Group

<sup>1</sup>Medical University Innsbruck  
<sup>2</sup>Oroboros, Innsbruck, Austria

### Aims

Clarity of concept and consistency of nomenclature facilitate effective transdisciplinary communication, education, and ultimately further discovery.

Adhering to uniform standards and harmonizing the terminology concerning mitochondrial respiratory states and rates will support the development of databases of mitochondrial respiratory function in cells, tissues, and species.

### Summary

Recommendations on coupling control states and rates are focused on studies with mitochondrial preparations.

**Fig. 1:** Respiration is defined by O<sub>2</sub> flux balance.

**Fig. 2:** OXPHOS analysis is based on the study of mt- preparations. Metabolic fluxes measured in defined coupling and pathway control states provide insights into the meaning of cellular respiration.

**Fig. 3:** Interpretation of respiratory rates depends critically on appropriate normalization.

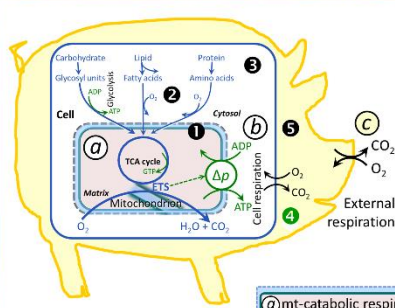
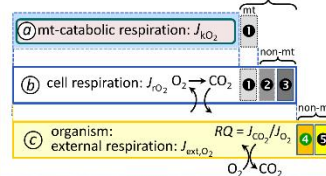


**Figure 1. From mitochondrial to external respiration**

Mitochondrial (mt) respiration is the oxidation of fuel substrates (electron donors) and reduction of O<sub>2</sub> catalysed by the electron transfer system, ETS:

- (a) mt-catabolic respiration, excluding
- (b) mt-residual oxygen consumption, *Rox*.
- (c) Total cellular O<sub>2</sub> consumption, including mt-*Rox*,
- (d) non-mt catabolic *Rox*, particularly by peroxisomal oxidases, and
- (e) non-mt *Rox* unrelated to catabolism.

External respiration, including aerobic microbial respiration, and extracellular O<sub>2</sub> consumption.



MiPart by Odra Noel

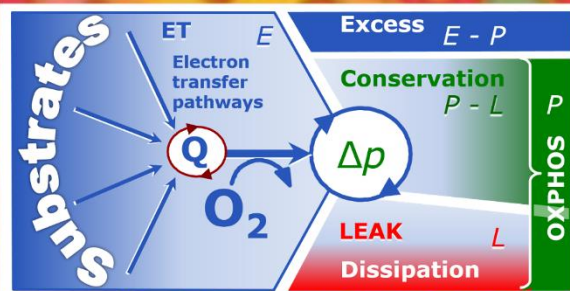


**Figure 2. Respiratory states (ET, OXPHOS, LEAK) and corresponding rates (E, P, L)**

Table 1. Coupling states and residual oxygen consumption in mitochondrial preparations in relation to respiration- and phosphorylation-flux,  $J_{kO_2}$  and  $J_{p_0}$ , and protonmotive force,  $\Delta p$ . Coupling states are established at kinetically saturating concentrations of fuel substrates and O<sub>2</sub>.

State	$J_{kO_2}$	$J_{p_0}$	$\Delta p$	Inducing factors	Limiting factors
LEAK	$L$ ; low, cation leak-dependent respiration	0	max.	proton leak, slip, and cation cycling	$J_{p_0} = 0$ : (1) without ADP, $L_S$ ; (2) max. ATP/ADP ratio, $L_T$ ; or (3) inhibition of the phosphorylation-pathway, $L_{Oxy}$
OXPHOS	$P$ ; high, ADP-stimulated respiration	max.	high	kinetically-saturating [ADP] and [P <sub>i</sub> ]	$J_{p_0}$ by phosphorylation-pathway; or $J_{kO_2}$ by ET-capacity
ET	$E$ ; max., noncoupled respiration	0	low	optimal external uncoupler concentration for max. $J_{O_2,E}$	$J_{kO_2}$ by ET-capacity
ROX	$Rox$ ; min., residual O <sub>2</sub> consumption	0	0	$J_{O_2,Rox}$ in non-ET-pathway oxidation reactions	inhibition of all ET-pathways; or absence of fuel substrates

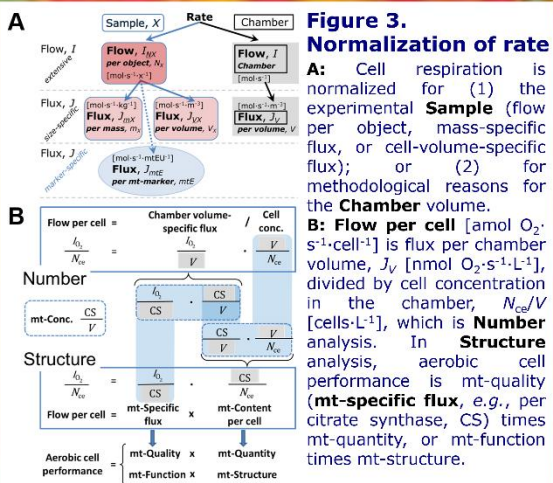


**Figure 3. Normalization of rate**

**A:** Cell respiration is normalized for (1) the experimental **Sample** (flow per object, mass-specific flux, or cell-volume-specific flux); or (2) for methodological reasons for the **Chamber** volume.

**B: Flow per cell** [amol O<sub>2</sub> s<sup>-1</sup> cell<sup>-1</sup>] is flux per chamber volume,  $J_V$  [nmol O<sub>2</sub> s<sup>-1</sup> L<sup>-1</sup>], divided by cell concentration in the chamber,  $N_{ce}/V$  [cells L<sup>-1</sup>], which is **Number** analysis. In **Structure** analysis, aerobic cell performance is mt-quality (mt-specific flux, e.g., per citrate synthase, CS) times mt-quantity, or mt-function times mt-structure.